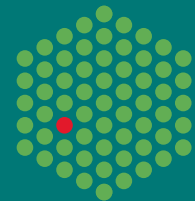


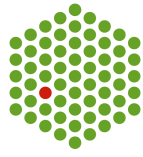
# Sample quality control for Structural Studies

Maria Garcia Alai  
EMBL Team Leader

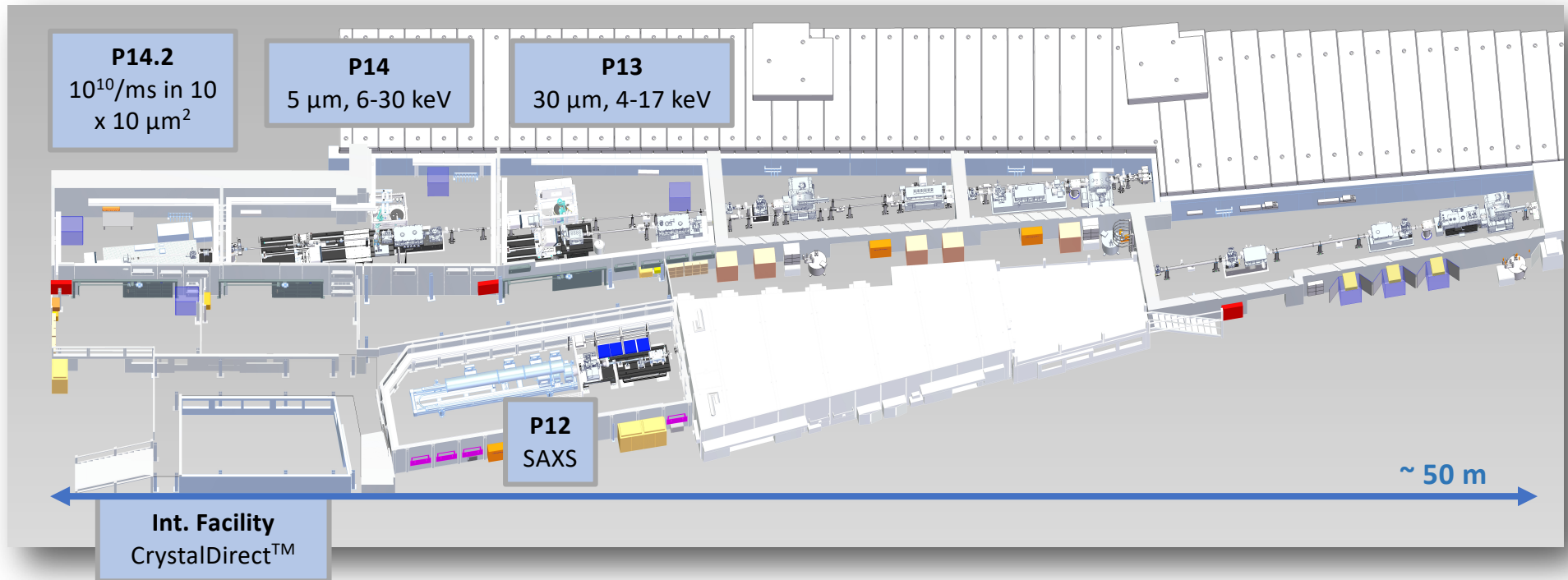
EMBL



25<sup>th</sup> Sep. 2019



## 3 Beamlines at PETRA III



- EMBL Hamburg operates the entire beamlines beginning at the 'frontend'
- The beamlines are embedded in the Integrated Facility for Structural Biology

## High-throughput crystallization



HTX

## Protein Characterization (Molecular Biophysics)



PC

# High-throughput Crystallization Facility

Screens

Robots

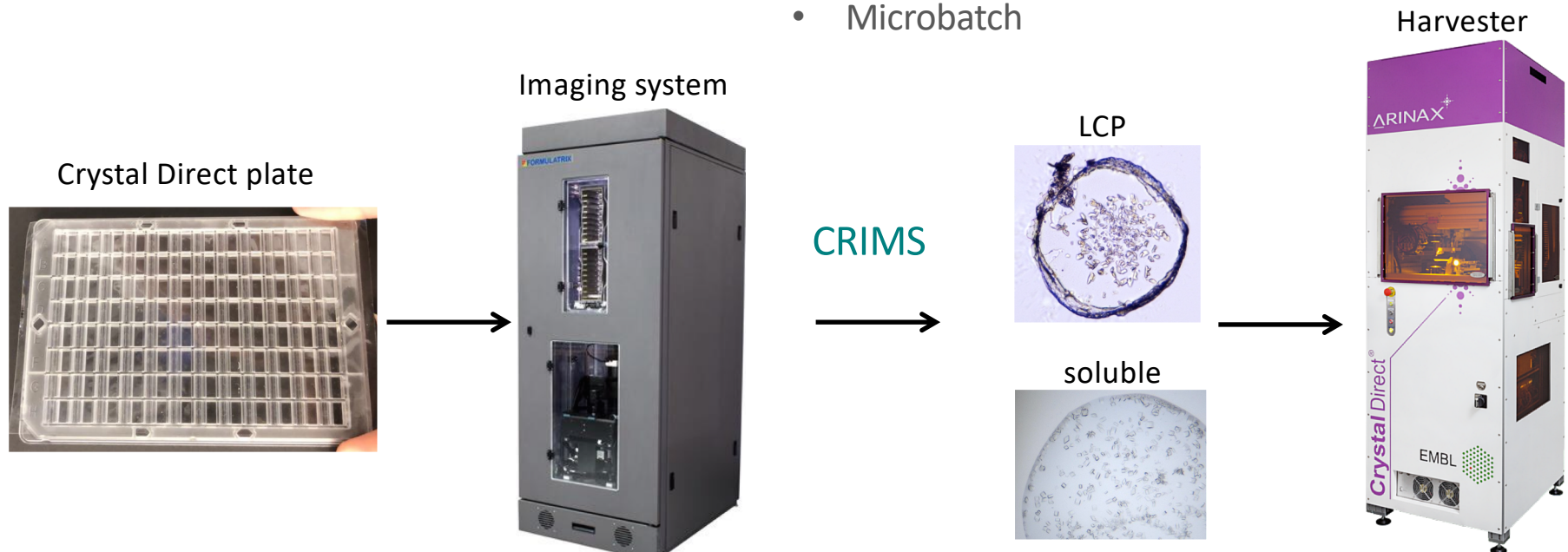
Plates

Imaging

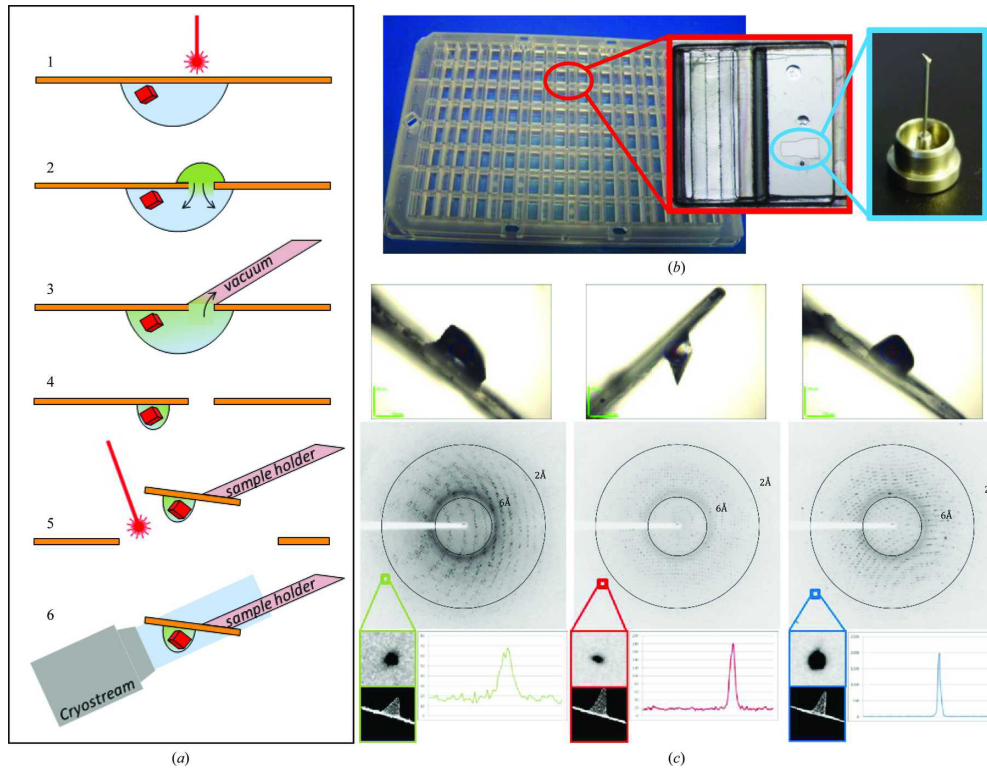
CRIMS



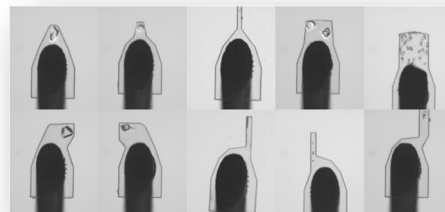
- Initial screening 16
- Optimization 13
- LCP
- Additive
- Customized screens
- 2 TTP mosquito
- Scorpion
- CrystalDirect
- Swissci
- Intelli
- LCP
- Hanging drop
- Microbatch
- Formulatrix
- 19 °C and 4 °C



# Crystal Direct Harvester



Zander et al. (2016). Automated harvesting and processing of protein crystals through laser photoablation. *Acta Cryst.* (2016). D72, 454-466



A robotic **CrystalDirect Harvester** (arinax.com) system for (remote) harvesting and cryo-cooling of crystals is operational

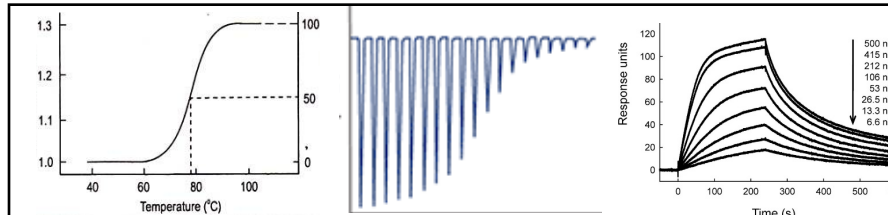
# Molecular Biophysics Platform

## Characterization

## Interaction

## Kinetics

iLAB



1. MS
2. TF
3. nDSF
4. DLS
5. CD
6. FT-IR

7. ITC
8. MST

9. SPR
10. Interferometry
11. Stopped-flow



8) Microscale Thermophoresis Monolith NT.115 and NT.LabelFree Nanotemper



10) Bioforte Octet Red96



9) Biacore T200 GE



6) Infrared spectroscopy Bruker Vertex 70



4) Differential light scattering Wyatt



7) Isothermal titration calorimetry MicroCal



11) Stopped-flow AppliedPhotophysics



5) Circular Dichroism AppliedPhotophysics



1) MALDI TOF: Bruker/CovalX



2) Thermofluor



3) Differential Scale Fluorimetry Prometheus 48 Nanotemper

# Outline:

---

- Quality control
- Protein Folding
- Biophysical characterization

# Quality control

---

-What does it mean “Protein quality control”  
And... why do we care?

# Quality control of purified proteins to improve research data reproducibility:

## Little pain, lots to gain?

ARBRE-MOBIEU (Association of Resources for Biophysical research in Europe – MOlecular BIophysic in EUrope) and P4EU (Protein Production and Purification Partnership in EUrope)

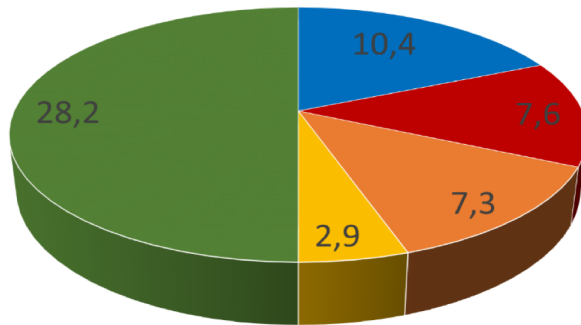


Figure 1. Categorization of preclinical research spending in the US into levels of reproducibility and common errors leading to data irreproducibility (2012 data, all figures in US \$billions, adapted with permission from reference (3)). The ‘Biological Reagents and Reference Materials’ category includes approximately \$0.5bn spent on poor quality commercial antibodies (4).

**Begley, C.G. & Ioannidis, J.P. Reproducibility in science: improving the standard for basic and preclinical research. *Circ. Res.* 116, 116-26 (2015).**

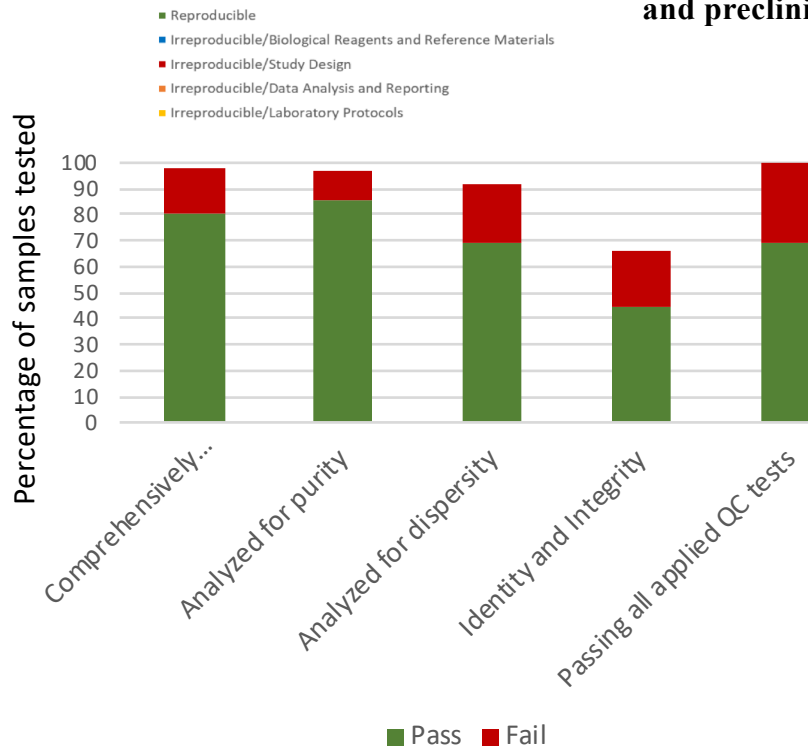


Figure 2. Summary of sample testing and results. ‘Comprehensively documented’ is an evaluation of the documentation supplied with the protein samples and reflects our opinion on whether this is sufficient to easily reproduce the sample. Samples ‘Analysed for Purity’ have been evaluated using SDS-PAGE, CE, RPLC or similar analytical techniques. Samples ‘Analysed for Dispersity’ were evaluated using SEC, DLS, SEC-MALS or Field-Flow Fractionation, Field-Flow Fractionation-MALS or Analytical Ultra-Centrifugation. Identity and Integrity was evaluated using MS (bottom up or top down as appropriate).

- 186 samples from 47 laboratories
- 30% samples failed at least in one QC test

# Quality control of purified protein

## Best practice recommendations

---

### **Guideline**

#### ii) Minimal quality control parameters that should be tested on protein sample

- Purity & integrity
- Homogeneity (aggregation state)
- Identity

#### iii) Extended quality control parameters

- General quality test by UV spectroscopy
- Homogeneity Conformational stability/folding state
- Optimization of storage conditions
- Batch-to-batch consistency

# Protein Folding

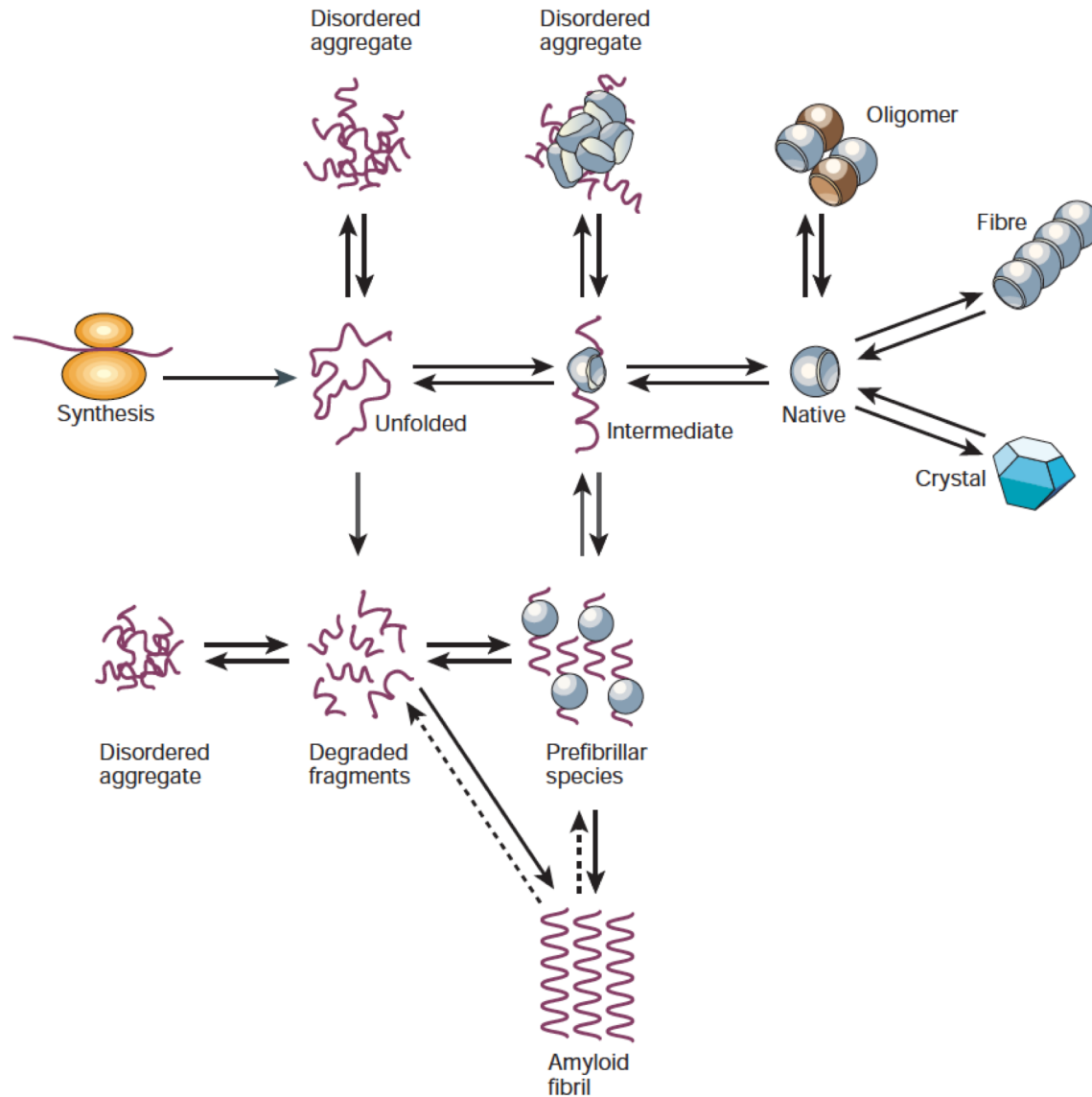
---

**$20^n$  different possible polypeptide chains of  $n$  amino acids long**

- It is estimated that there are between  $10^{78}$  to  $10^{82}$  atoms in the known, observable universe.

**Only a very small fraction of this vast set of conceivable polypeptide chains would adopt a single, stable three-dimensional conformation—by some estimates, less than one in a billion.**

# Protein folding



## Quiz:

---

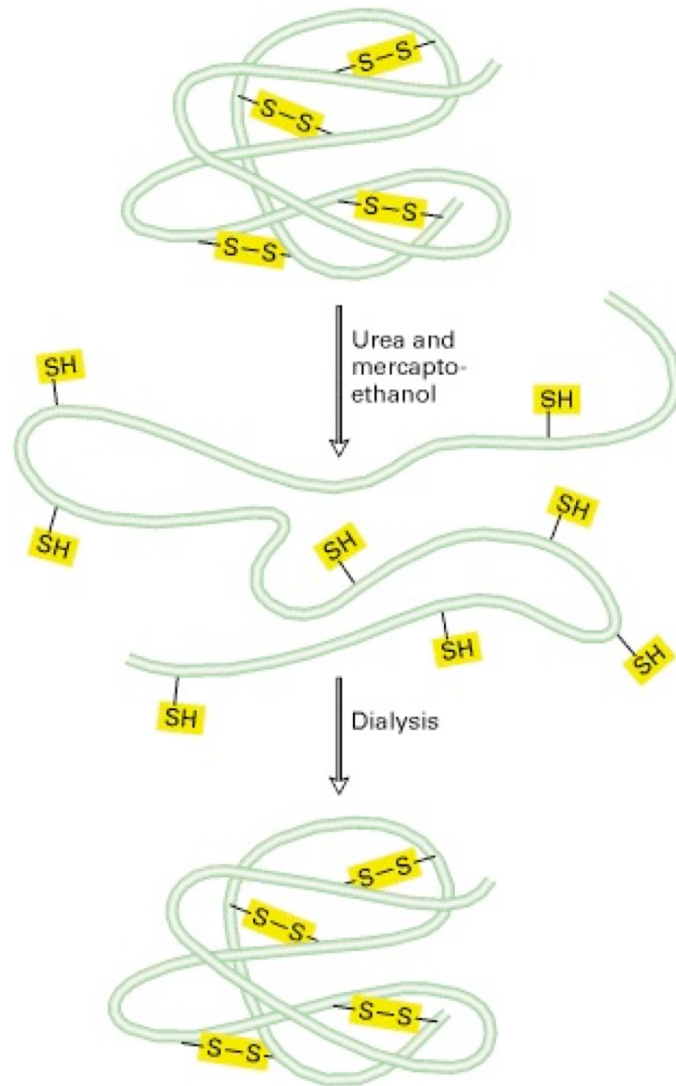
- Who has ever done a refolding experiment?

## Quiz:

---

- Who has ever done a refolding experiment?
- Who has ever done a mini-prep?

# In vitro denaturation and renaturation of proteins



Ribonuclease

## Christian Anfinsen's experiment

- Treatment with an 8 M urea solution containing mercaptoethanol completely denatures most proteins.
- The urea breaks intramolecular hydrogen and hydrophobic bonds, and the mercaptoethanol reduces each disulfide bridge ( $-S-S-$ ) to two sulfhydryl ( $-SH$ ) groups.
- When these chemicals are removed by dialysis, the  $-SH$  groups on the unfolded chain oxidize spontaneously to re-form disulfide bridges, and the polypeptide chain simultaneously refolds into its native conformation and activity is reestablished.

**Nobel prize in Chemistry 1972**

# The thermodynamic hypothesis

---

”3D structure of a native protein in its normal physiological milieu (solvent, pH, ionic strength, presence of other components such as metal ions or prosthetic groups, temperature, etc.) is the one in which the **Gibbs free energy** of the *whole system* is **lowest**”

- the native conformation is determined by the totality of interatomic interactions and hence by the amino acid sequence, in a *given environment*.
- In terms of natural selection: a protein molecule only makes stable, structural sense when it exists under conditions similar to those for which it was selected “the so-called physiological state”.

# The Two-states model

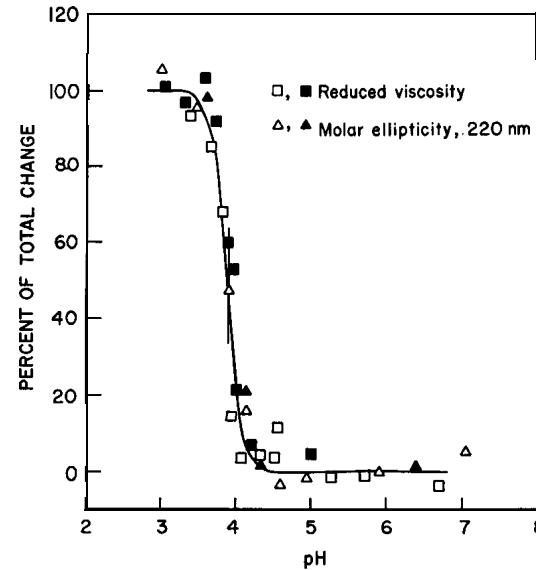
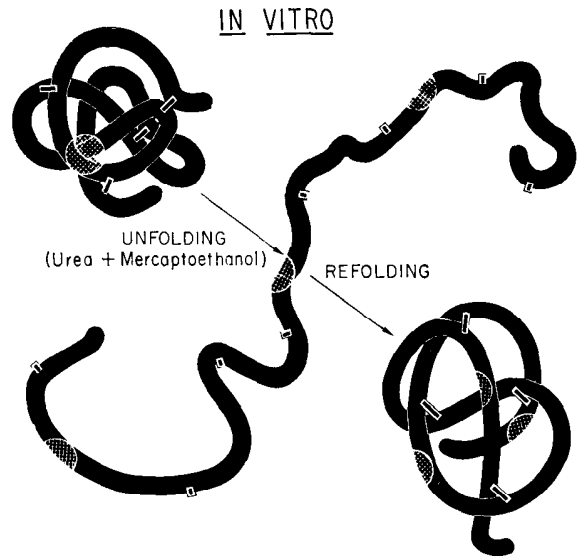
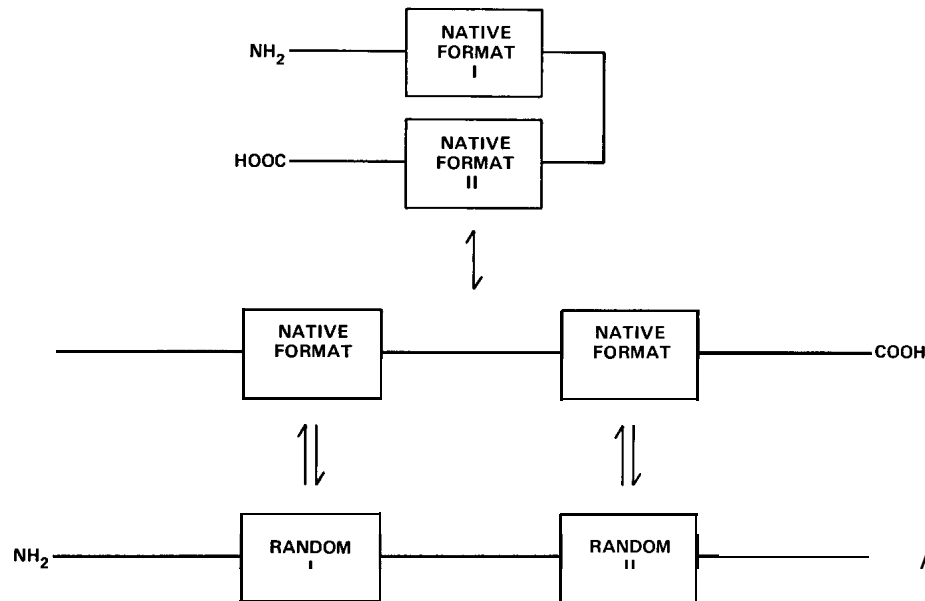
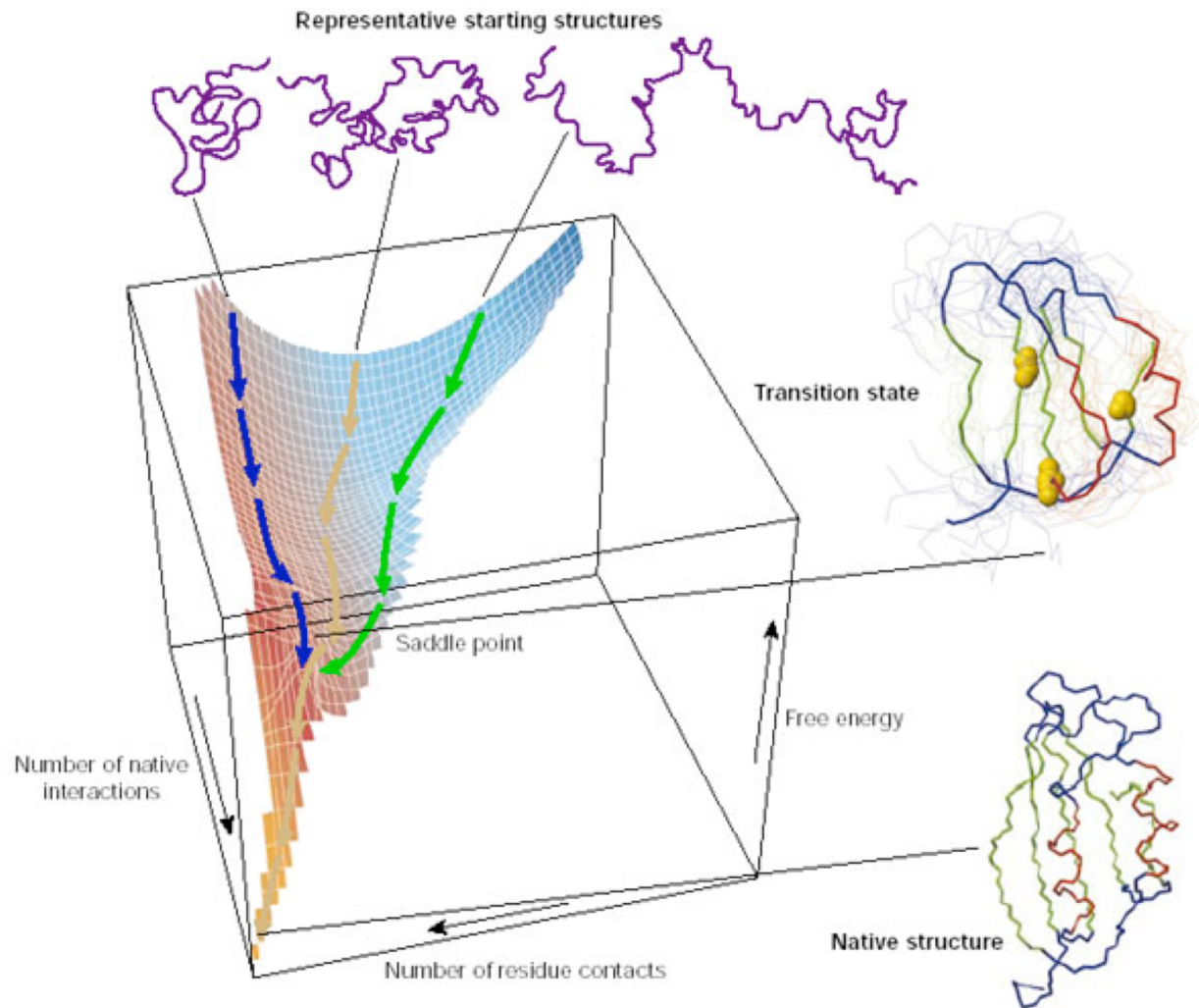


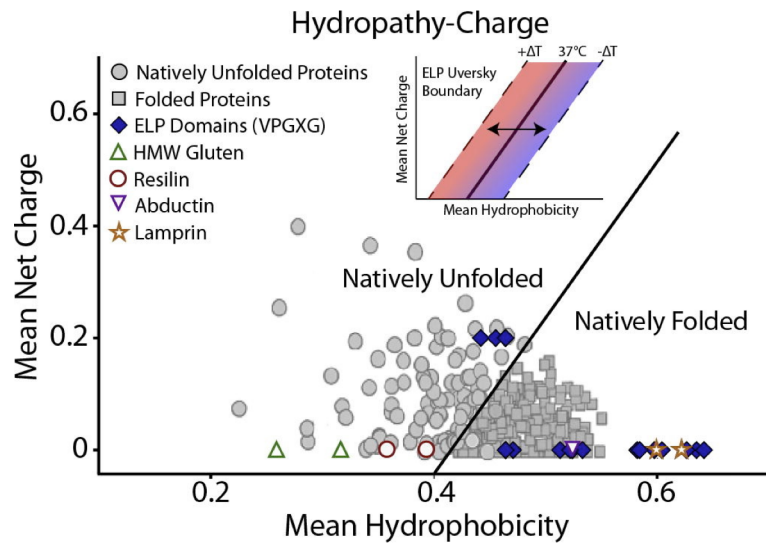
Fig. 9. Changes in reduced viscosity and molar ellipticity at 220 nm during the acid-induced transition from native to denatured nuclease. □ and ■, Reduced viscosity; △ and ▲, molar ellipticity at 220 nm. □ and △, Measurements made during the addition of acid; ■ and ▲, measurements made during the addition of base. A. N. Schechter, H. F. Epstein and C. B. Anfinsen, unpublished results.



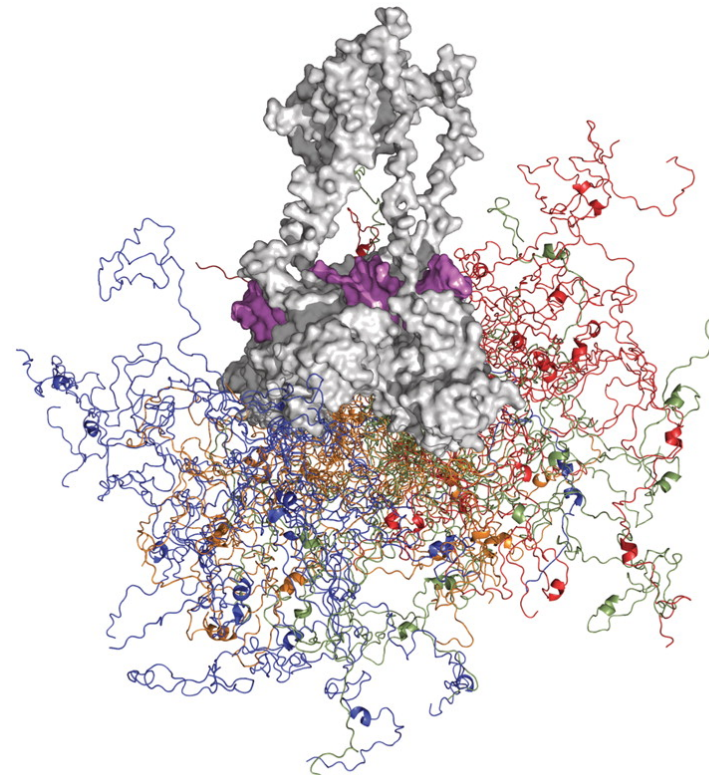
# The critical region: the transition state



# Intrinsically disordered proteins



Roberts S1, Dzuricky M2, Chilkoti A1. FEBS Lett. 2015 Sep 14;589(19 Pt A):2477-86.



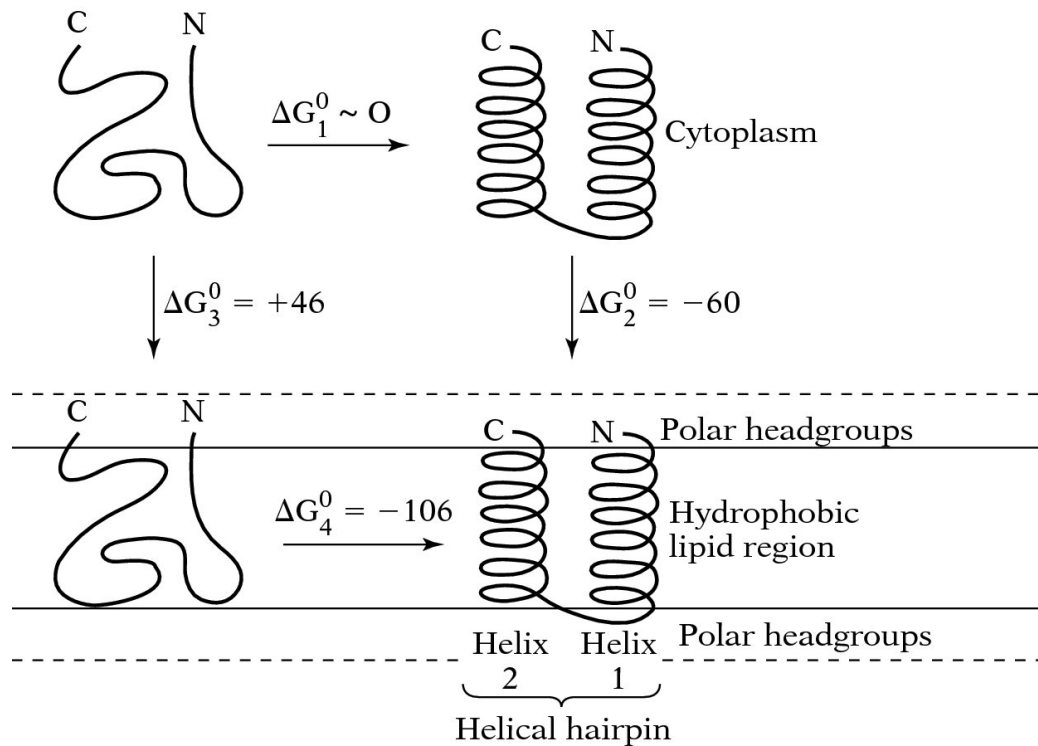
Mark Wells et al. PNAS 2008;105:5762-5767

## How to study them?

- Bioinformatics
- SAXS
- CD
- NMR

# Protein folding on membrane proteins

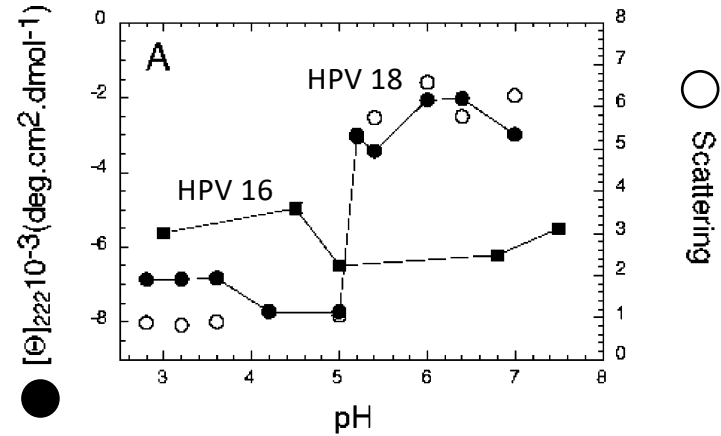
## Folding $\alpha$ -helical membrane proteins



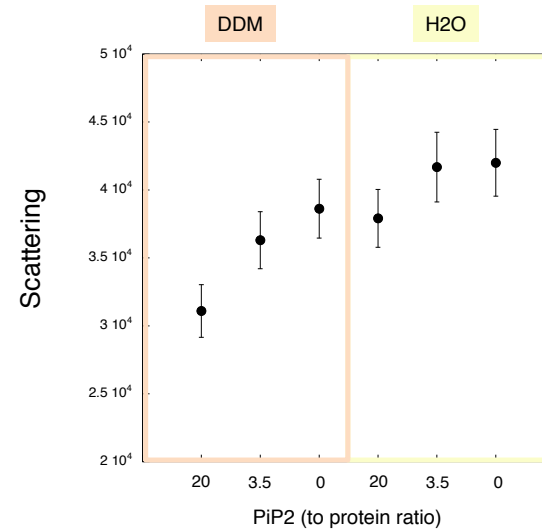
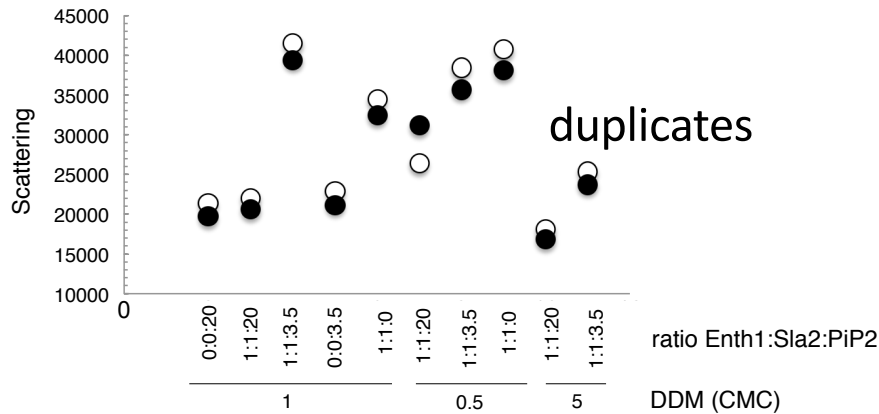
- Helical hairpin hypothesis
- Insertion of a hairpin structure composed of two helices into the nonpolar interior of the bilayer
- Insertion is driven by free energy arising from burying hydrophobic helical surfaces
- Alternative pathway of inserting unfolded peptide/random coil is energetically unfavored

# Sampling Protein Folding

- Solubility
- Aggregation
- Secondary structure contain
- Stability



light scattering at 360 nm (Fluorimeter)

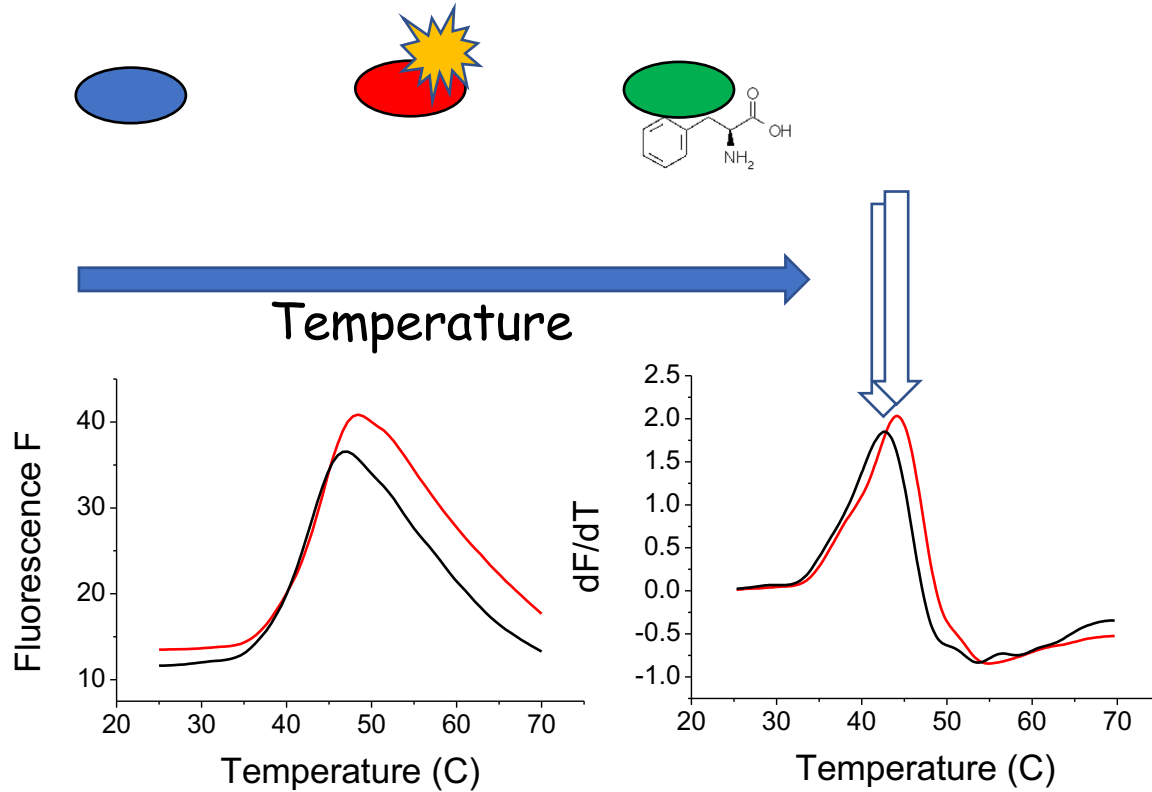


# Sampling Protein Folding

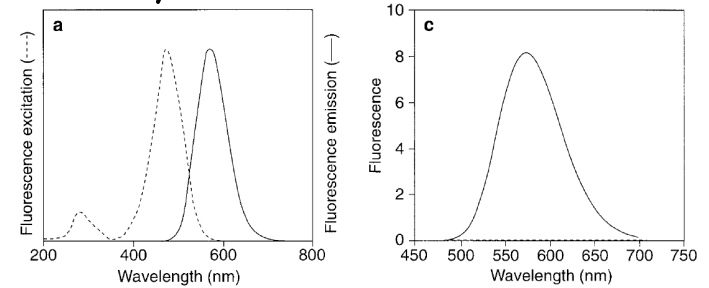
---

- Solubility
- Aggregation
- Secondary structure contain
- **Stability**
  - Screen for protein Stability

# Differential Scanning Fluorimetry



## ANS, bis-ANS

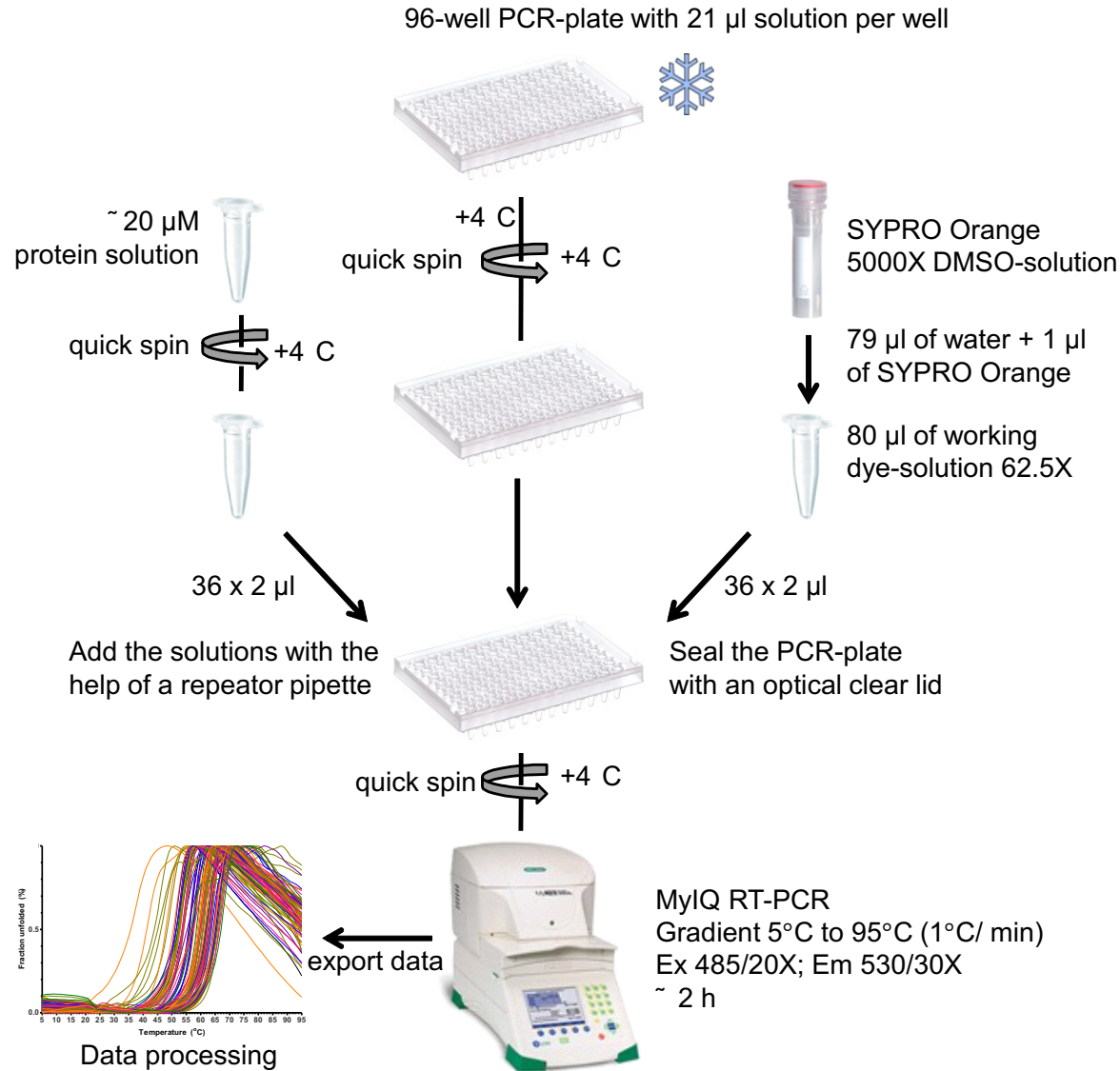


SYPRO Orange, Mol. Probes,  
Steinberg et al Anal. Biochem. 1996

Pantoliano et al J Biomol Screen. 2001

48- 96 samples

# Thermofluor



# Thermofluor

Sypro Orange/ ANS fluorescent properties will change as it binds to hydrophobic regions on the protein surface

## 8-anilino, 1-naphthalene sulfonate

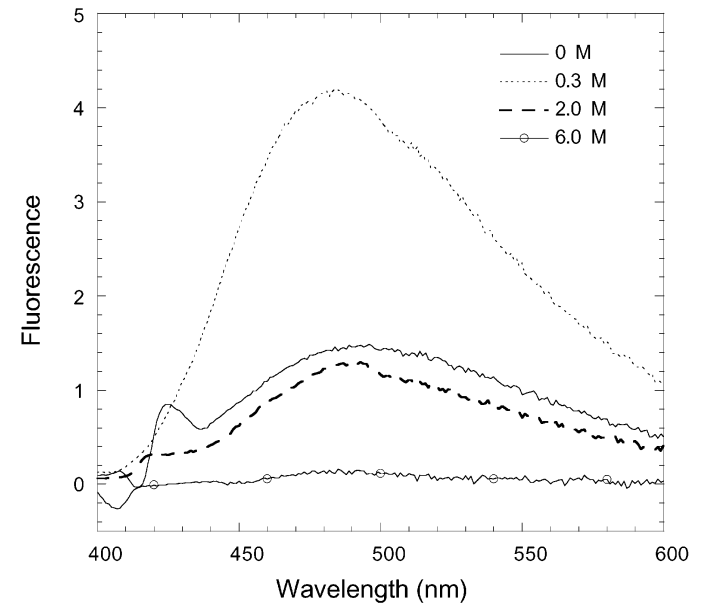
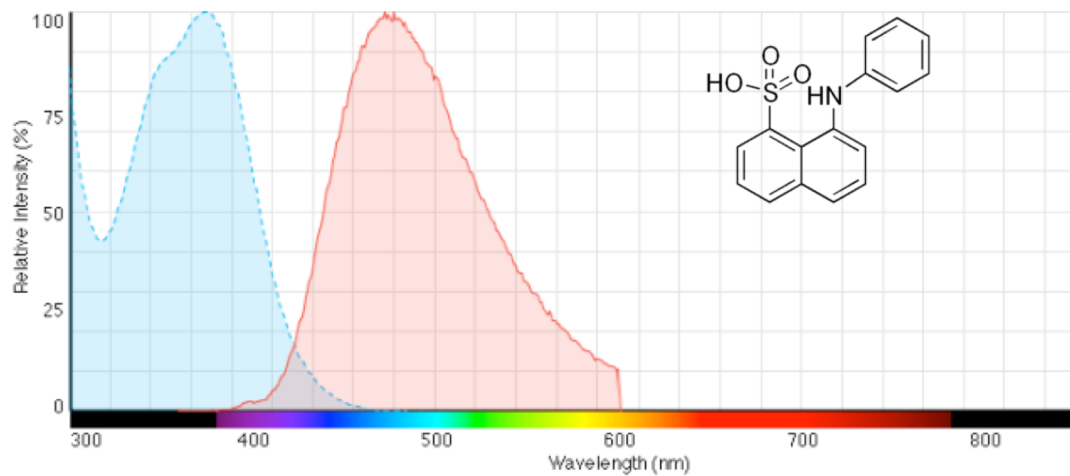
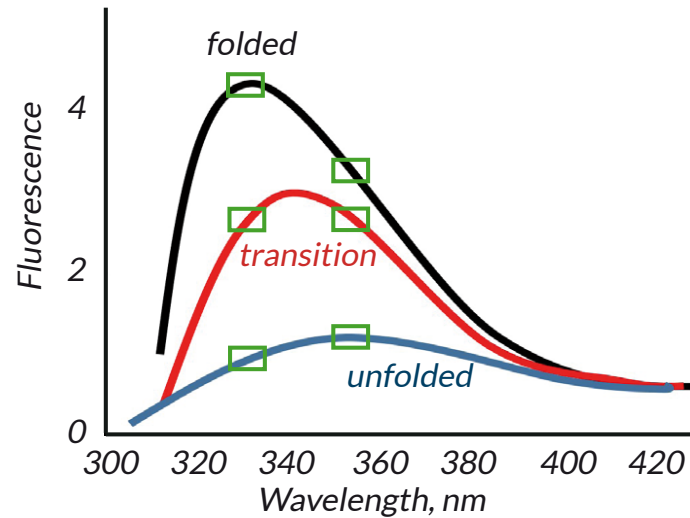
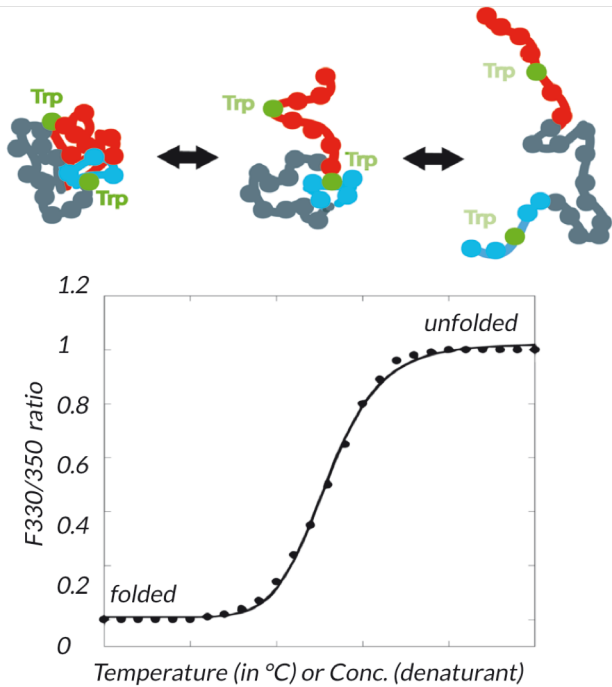


FIGURE 7: ANS binding of E7 after the GdmCl-induced conformational transition at the different denaturant concentrations indicated.

Not compatible with detergents!!!

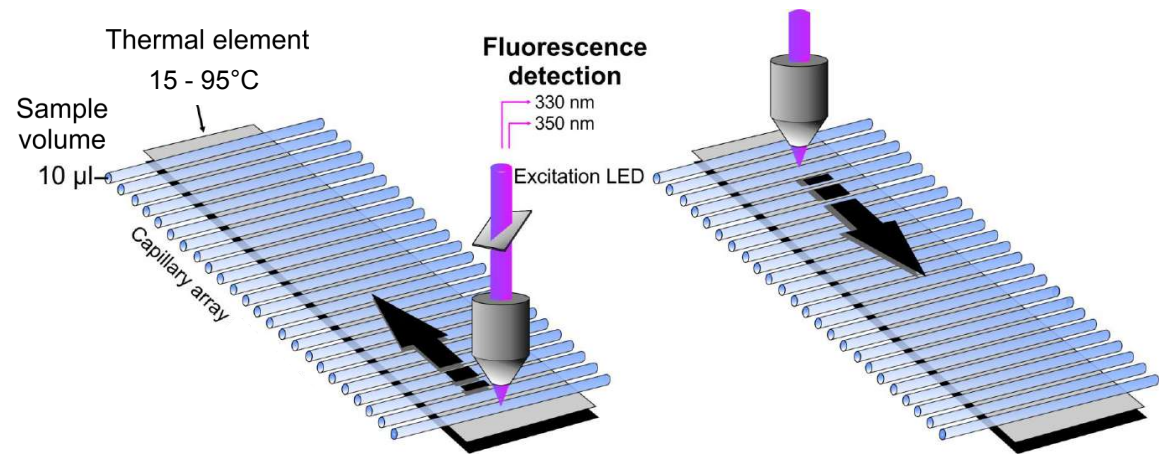
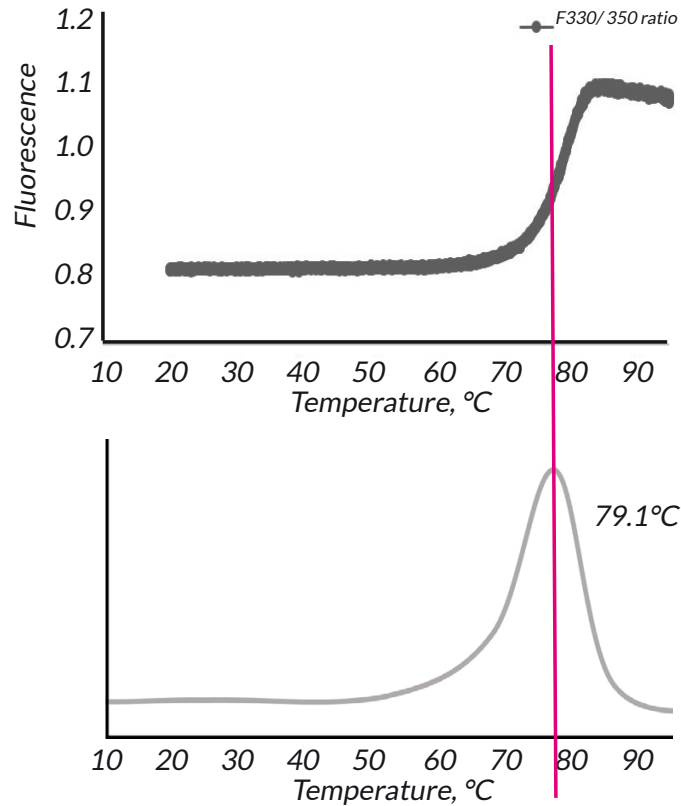
# nanoDSF

NanoTemper Technologies Prometheus NT.48



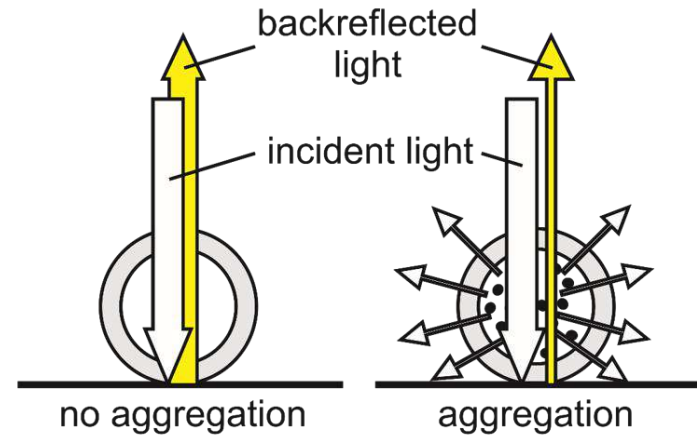
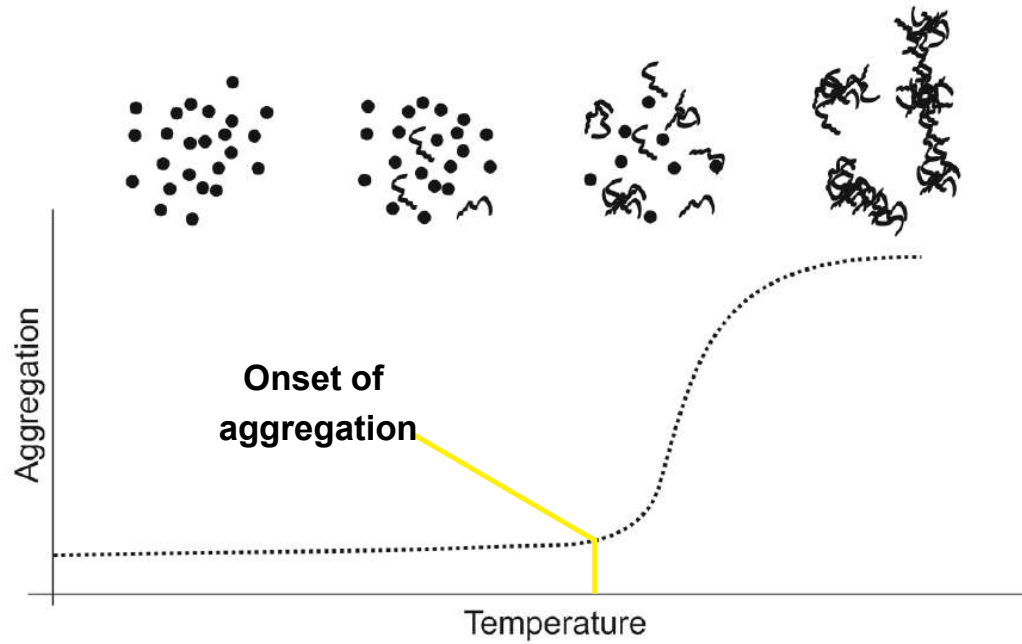
**Principle behind the nanoDSF.** Increasing temperature causes protein unfolding that can be assessed by monitoring changes of tryptophan fluorescence at 330nm and 350nm wavelength.

# The thermal unfolding transition midpoint ( $T_m$ )



- ratio  $F_{330}/350$  against the temperature
- $T_m$  is determined by first derivate analysis

# Static light scattering



# High-throughput screening for IMPs stability

---

40% samples processed in the SPC are membrane proteins

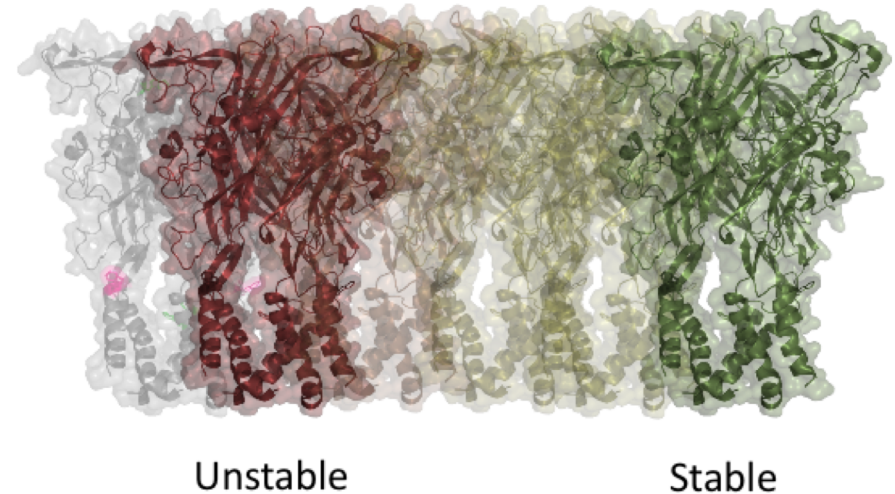
## **Introduction**

- IMP stability in detergent or membrane-like environments is the bottleneck for structural studies
- Detergent solubilization from membranes is usually the first step in the workflow
- Looking for a simple high-throughput screening method to identify optimal conditions for membrane protein stabilization

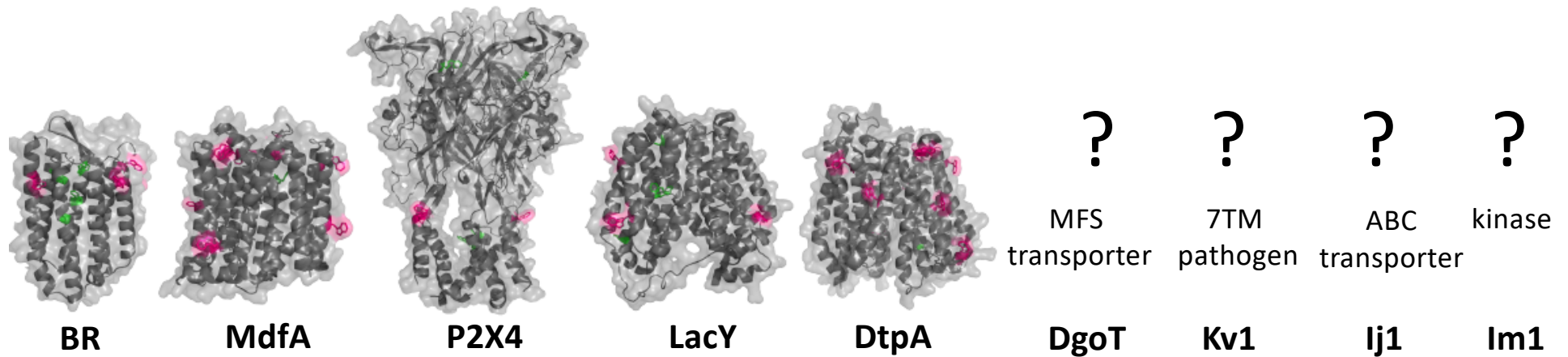
# High-throughput screening for IMPs stability

- following **nDSF and scattering** upon thermal denaturation
- (de-)stabilization **effects of detergents**
- find **suitable conditions** for downstream handling during purification
- **thermodynamic parameters (T<sub>m</sub>, Tagg, Tonset)**
- We selected 9 IMPs to benchmark our protocol

## Objective

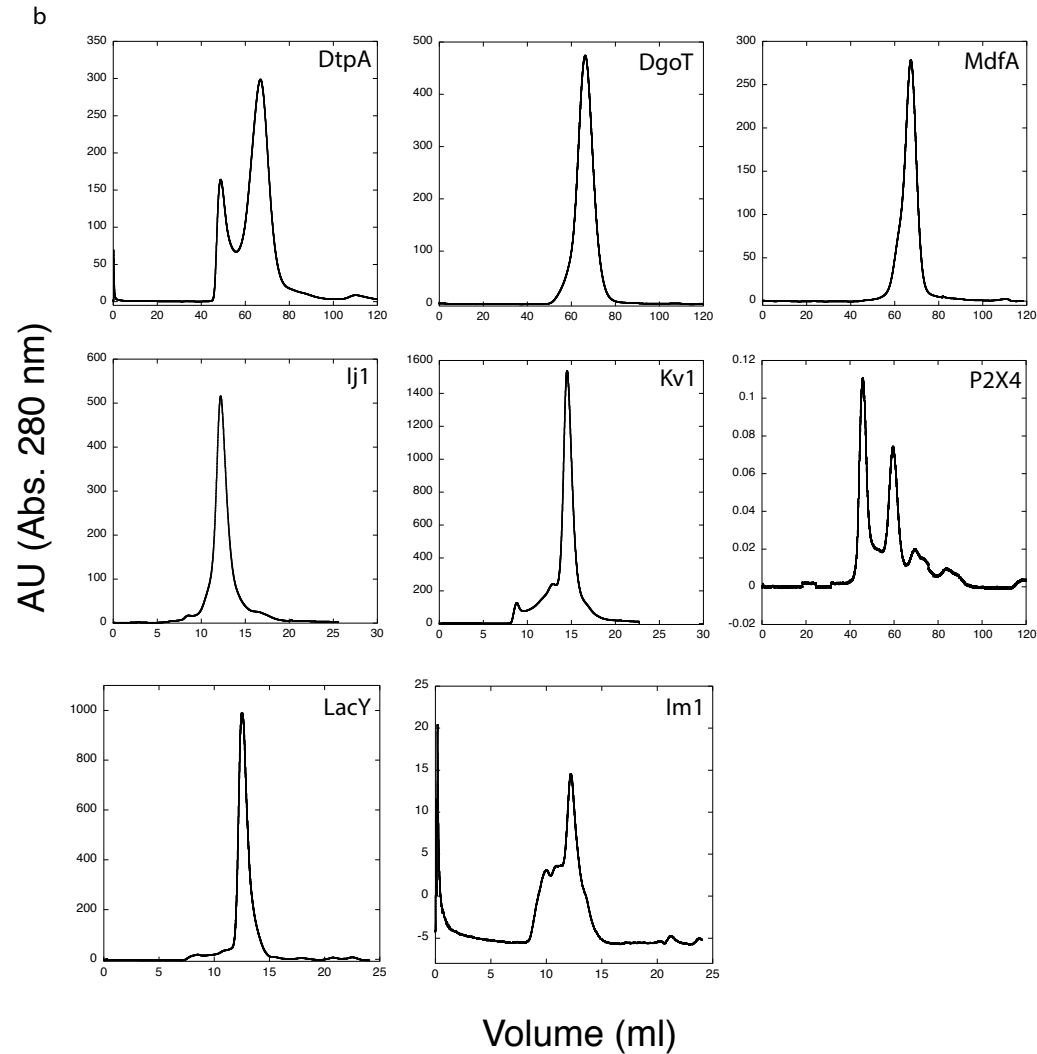
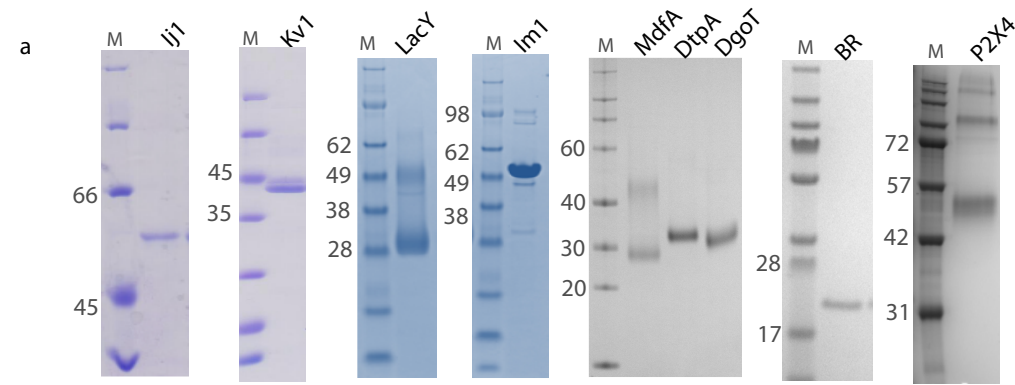


# We selected 9 Integral membrane proteins (targets)

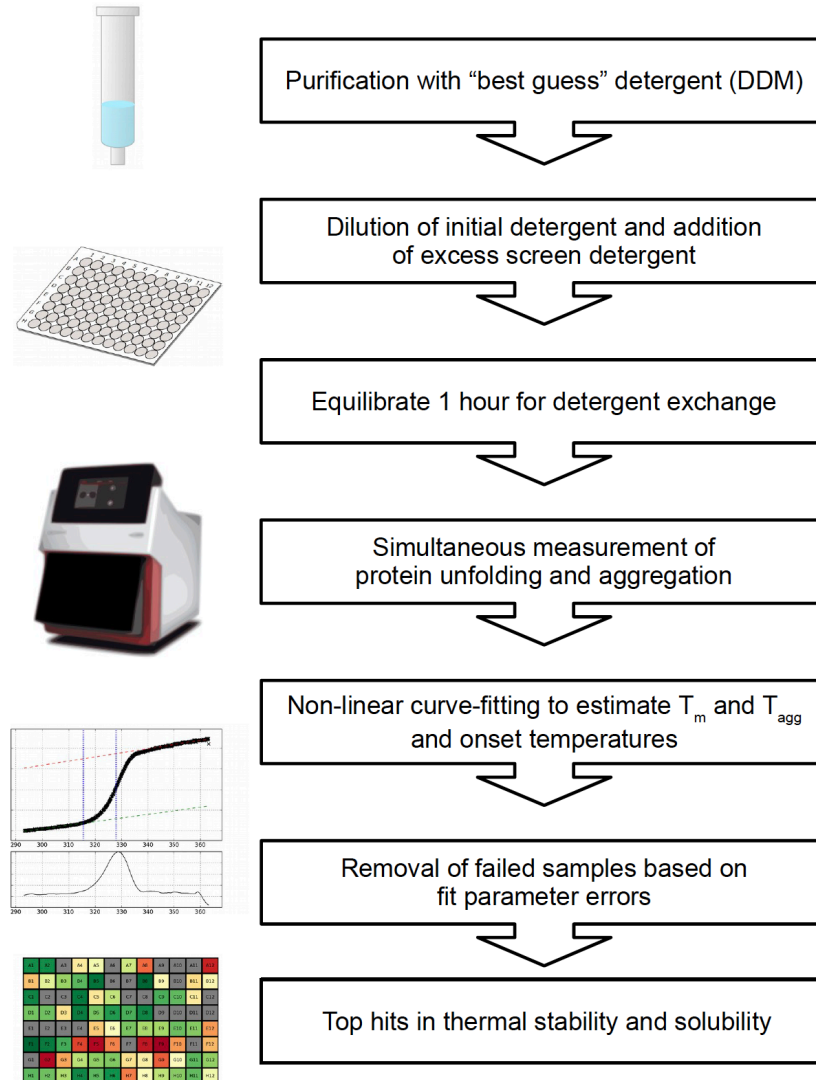


Protein	Organism	Family	Function	Number of Trp residues	PDB ID
DgoT	<i>E. coli</i>	MFS transporters	putative galactonate transporter	14	6E9N, 6E9O
MdfA	<i>E. coli</i>	MFS transporter	multi drug resistance	9	4ZP0, 4ZOW, 4ZP2, 6GV1, 6EUQ
DtpA	<i>E. coli</i>	MFS transporter	peptide transporter	10	6GS1, 6GS4, 6GS7
Kv1	<i>Pseudomonas aeruginosa</i>	unknown	unknown	17	—
Ij1	<i>E. coli</i>	ABC-Transporter	ion transport	22	—
P2X4	<i>Homo sapiens</i>	P2X ionotropic receptors	regulator in mediating neuropathic pain	6	4DW0, 4DW1 (zebrafish)
BR	<i>Halobacterium salinarum</i>	7TM receptor	proton pump	8	4MD1, 4MD2, 4XXJ
LacY	<i>E. coli</i>	MFS transporter	transport of beta-galactosides	5	1PV6
Im1	<i>E. coli</i>	HisKA	Kinase	2	—

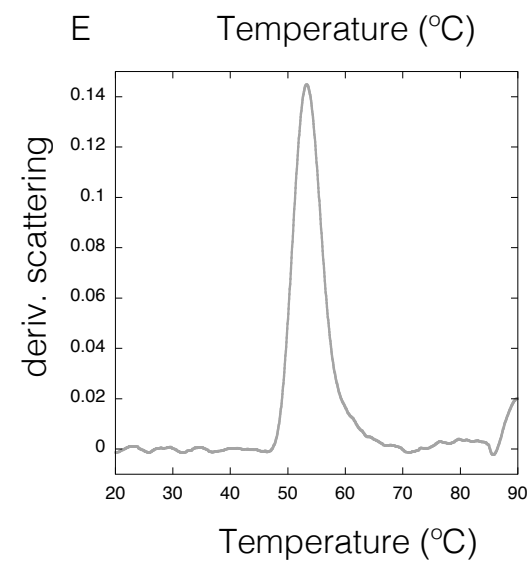
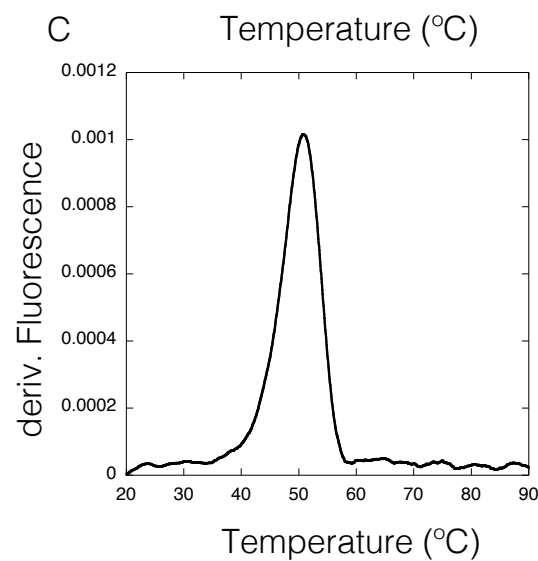
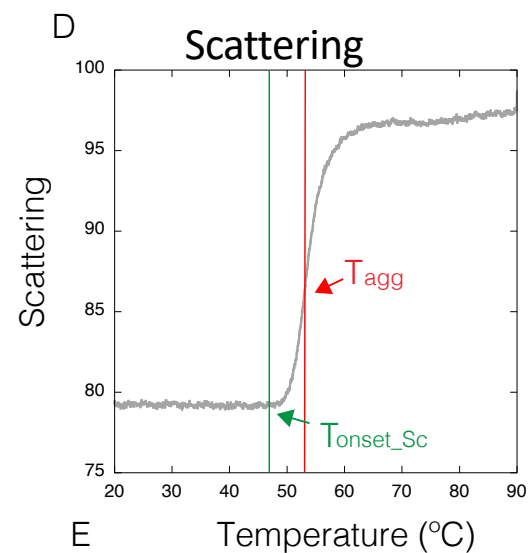
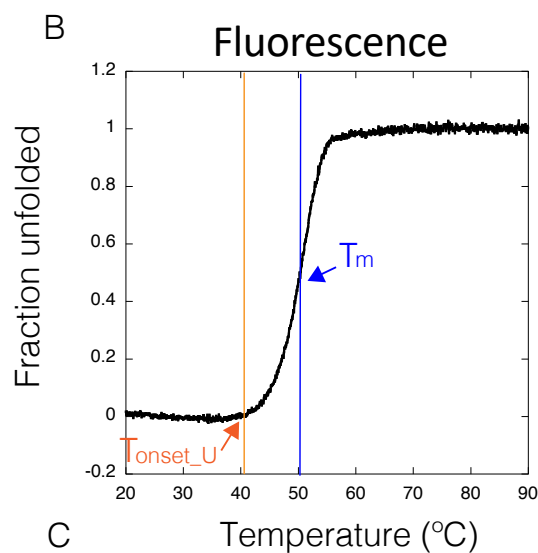
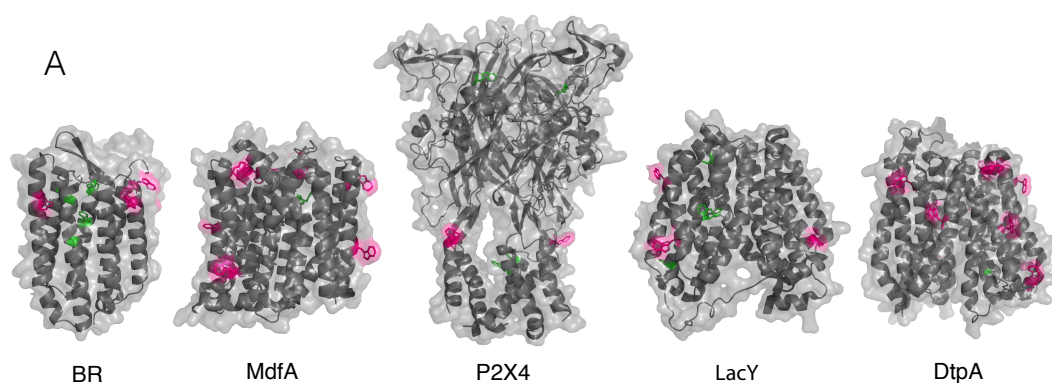
- Membranes solubilized in 1–2% DDM
- DDM as starting detergent in SEC



# Our pipeline

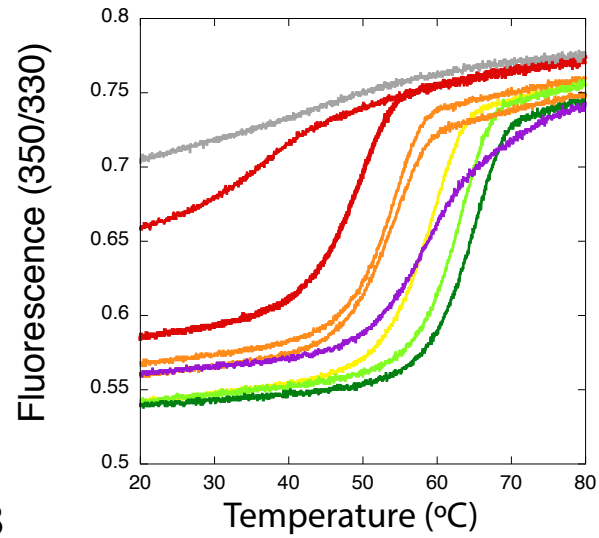


nDSF  
measurements

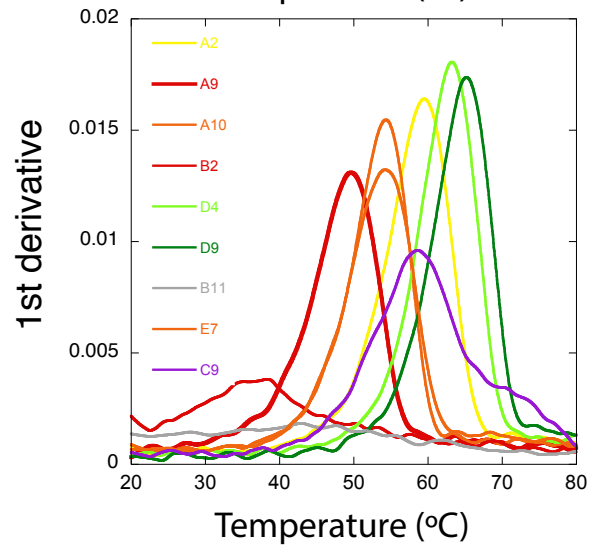


# Tm vs Tonset

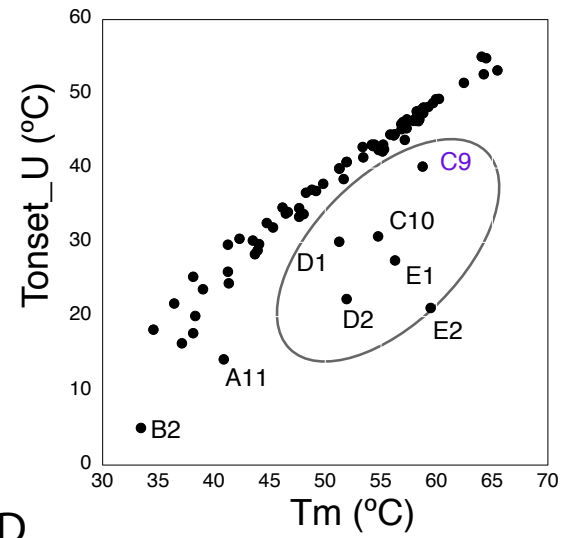
A



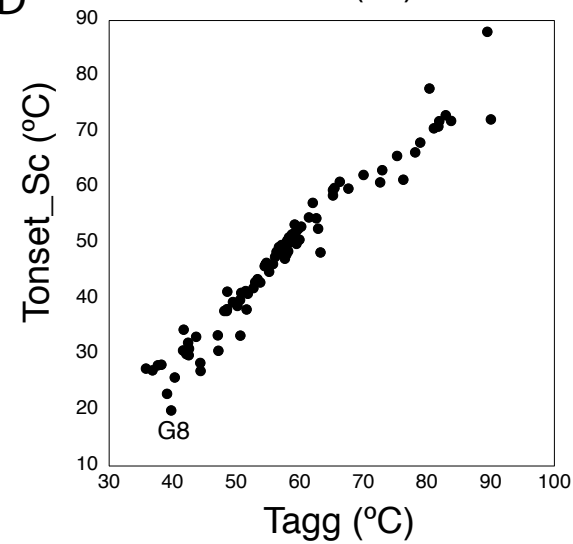
B



C



D



# Correlation between IMP stability and micelle size

Sample	Readout	n	Spearman's $\rho$
DtpA	Ratio	21	0.70
	Scattering	27	0.24
DgoT	Ratio	15	0.43
	Scattering	33	0.25
LacY	F330	8	0.00
	Scattering	27	-0.04
Kv1	Ratio	38	0.46
	Scattering	37	0.66
Ij1	Ratio	8	0.45
	Scattering	29	0.65
Im1	Ratio	9	0.78
MdfA	Ratio	33	0.74
	Scattering	36	0.20
P2X4	Ratio	42	0.80
BR	F330	28	0.84
	Scattering	28	0.73

Coefficients approaching zero show no correlation between variables while those approaching 1 indicate a positive correlation (Y values increase as the X values increase).

# Correlation between IMP stability and micelle size

Sample	Readout	n	Spearman's $\rho$
DtpA	Ratio	21	0.70
	Scattering	27	0.24
DgoT	Ratio	15	0.43
	Scattering	33	0.25
LacY	F330	8	0.00

**Regarding crystallization, shorter chain detergents are preferred as they allow for better crystal packing and better diffracting crystals. The goal is to find the shortest possible detergent that does not cause the protein to unfold!**

ImI	Ratio	9	0.78
MdfA	Ratio	33	0.74
	Scattering	36	0.20
P2X4	Ratio	42	0.80
BR	F330	28	0.84
	Scattering	28	0.73

Coefficients approaching zero show no correlation between variables while those approaching 1 indicate a positive correlation (Y values increase as the X values increase).

# Discussion

---

## **Implications for sample optimization**

- Analyse stability and solubility of IMPs by diluting them from their initial solubilization condition into different detergents
- Identify groups of detergents with characteristic stabilization and destabilization effects for selected targets
- Fos-choline and PEG family detergents may lead to membrane protein destabilization and unfolding
- Finding conditions that are suitable for downstream handling of membrane proteins during purification

# Absorption Spectroscopy

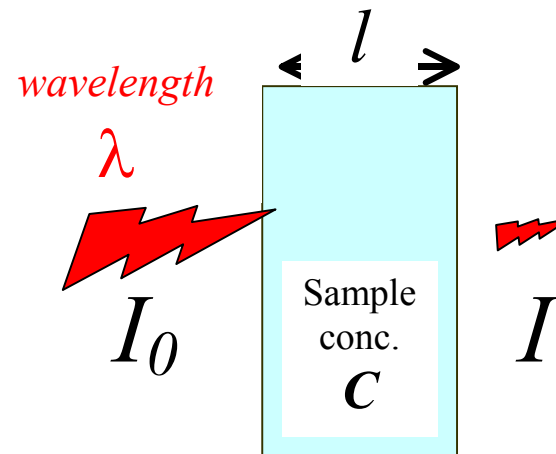
- Shine light through a sample and measure the proportion absorbed as a function of wavelength.

- Absorbance  $A = \log(I_0/I)$

- Beer-Lambert law:

$$A(\lambda) = \varepsilon(\lambda)lc$$

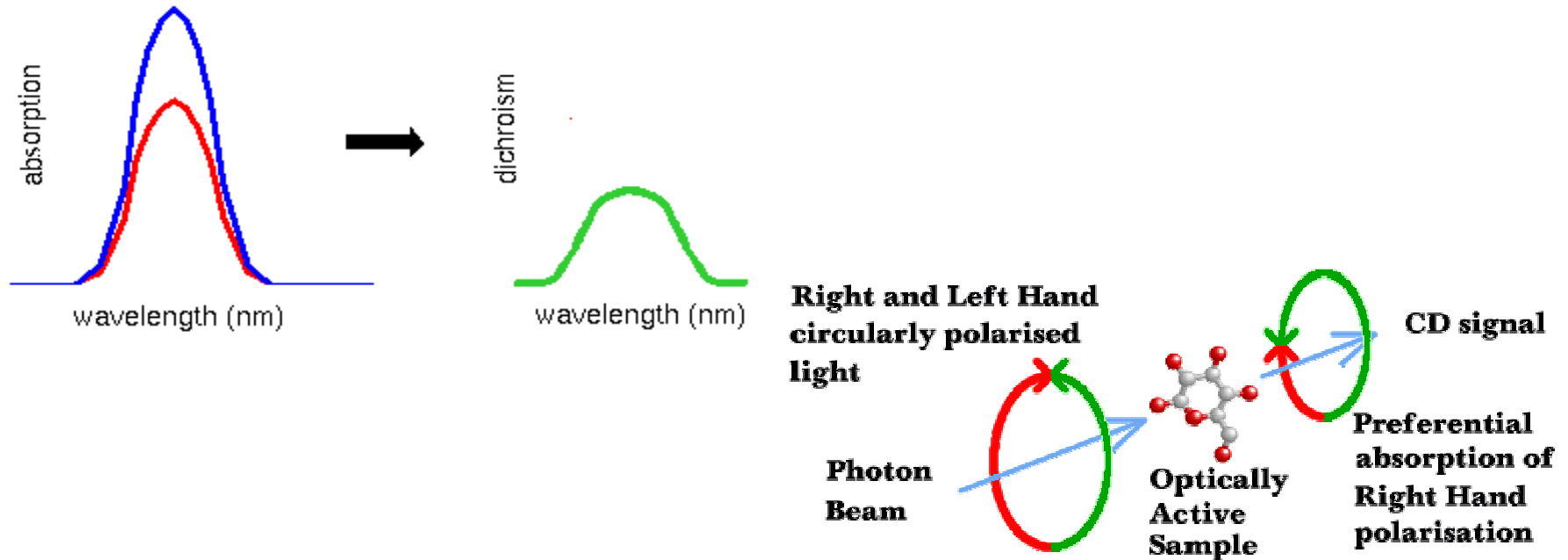
$\varepsilon$ : extinction coefficient



- The longer the path or the more concentrated the sample, the higher the absorbance

# Circular Dichroism

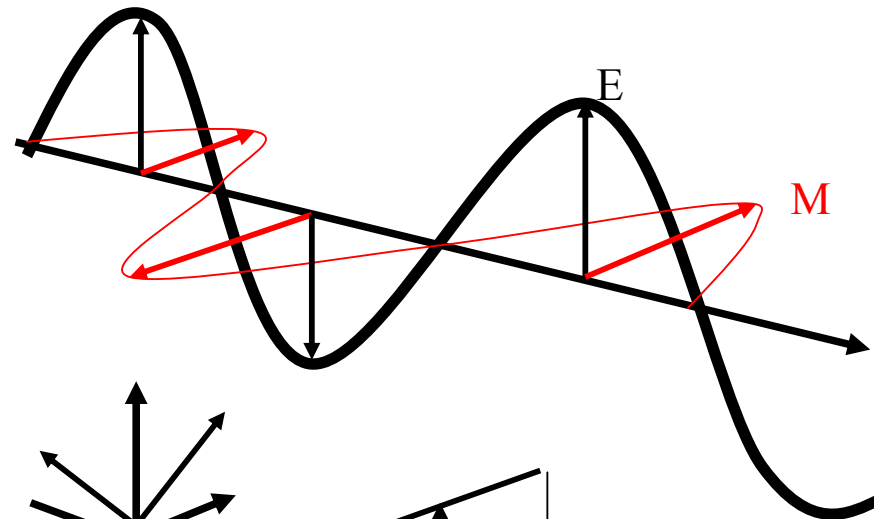
- CD measures the **difference** between the absorption of **left** and **right** handed circularly-polarized light. polarized light:



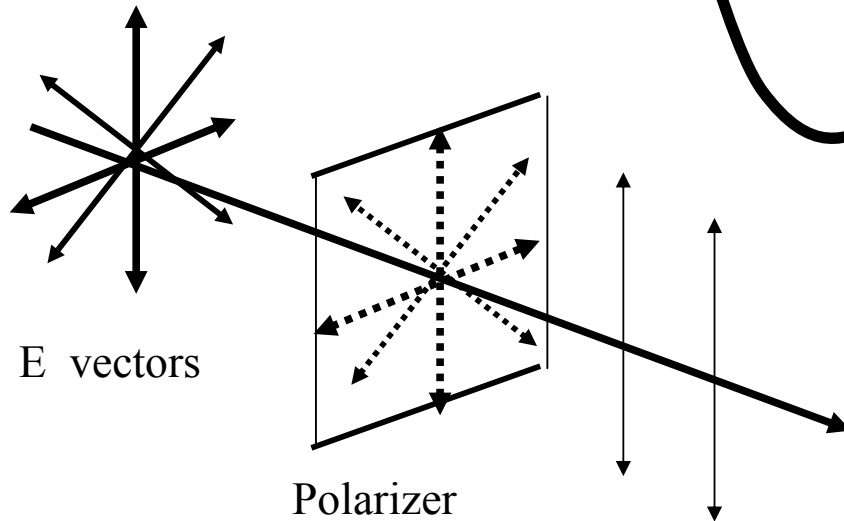
- This is measured as a function of wavelength, & the difference is always very small ( $\ll 1/10000$  of total). After passing through the sample, the L & R beams have different amplitudes & the combination of the two unequal beams gives elliptically polarized light. Hence, CD measures the ellipticity of the transmitted light (the light that remains that is not absorbed):

# Circular Dichroism

## Plane Polarized Light



Direction of propagation

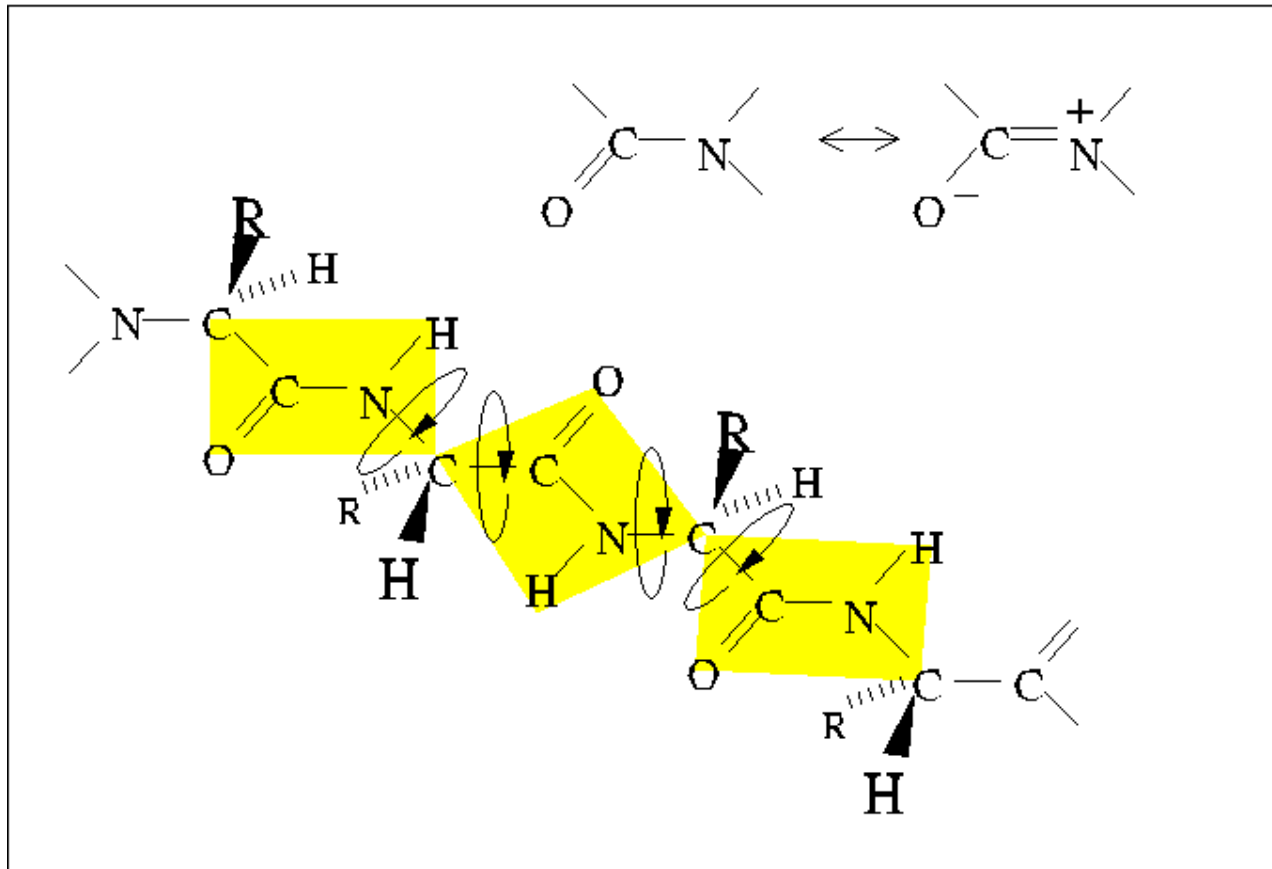


Direction of propagation

**Quarter-Wave Plate** at  $45^\circ$  to the optic axis, then the light is divided into two equal electric field components. One of these is retarded by a quarter wavelength by the plate (a net phase shift of  $\pi/2$ ). This **produces circularly polarized light.**

# Circular Dichroism

- The peptide bond is inherently asymmetric & is always optically active.
- Any optical activity from side-chain chromophores is induced & results from interactions with asymmetrical neighbouring groups.



# Units

- Molar Ellipticity

$$[\theta] = \frac{\theta}{c.l} \text{ deg cm}^2 \text{ dmol}^{-1}$$

$$[\theta] = \frac{\theta.M}{10.C.l} \text{ deg cm}^2 \text{ dmol}^{-1}$$

$$[\theta] = 3300 (\epsilon_L - \epsilon_R) = 3300 \frac{(A_L - A_R)}{Cl}$$

- Differential absorbance

$$\Delta\epsilon = \epsilon_L - \epsilon_R = \frac{[\theta]}{3300} M^{-1} \text{ cm}^{-1}$$

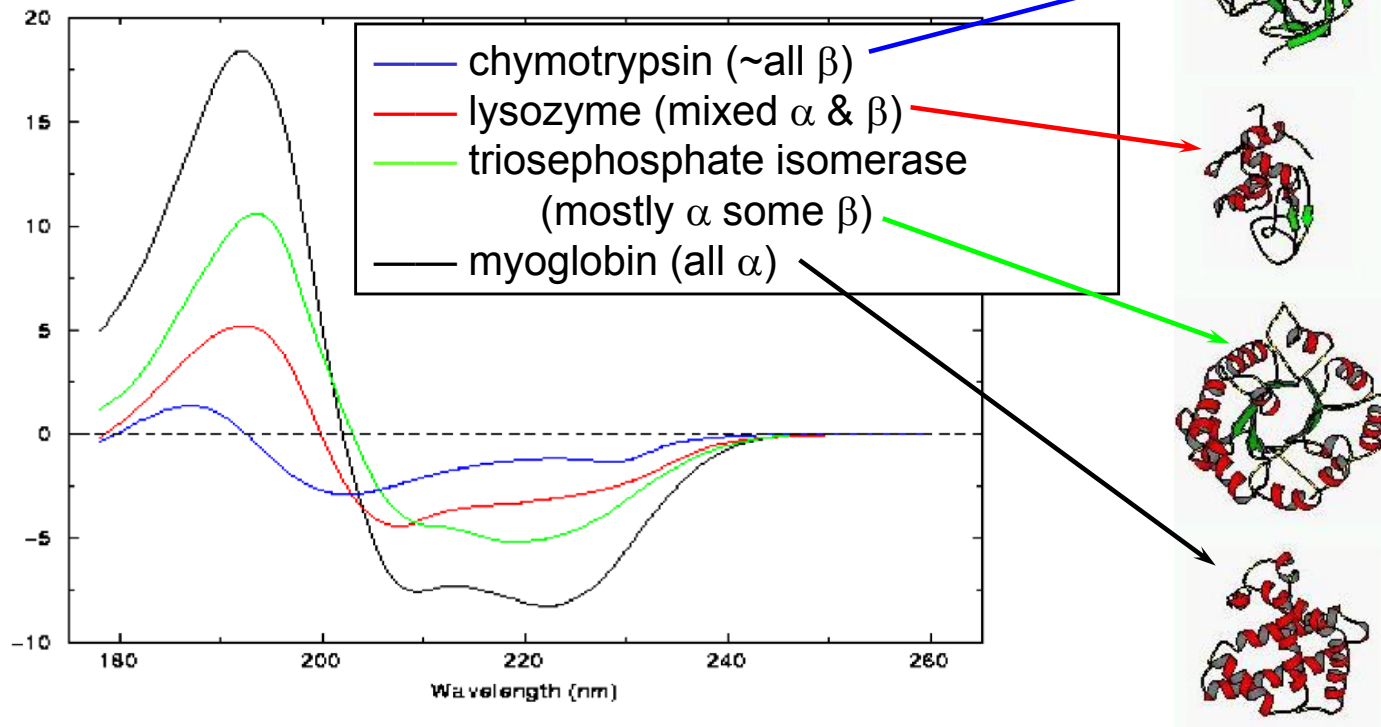
- $[\theta]$  and  $\Delta\epsilon$  can also be expressed per residue and this is useful for comparing systems of differing size
- $\theta$ ; signal millidegree,  $c$ ; [sample]  $\text{dmol L}^{-1}$ ,  $C$ ; [sample]  $\text{mg mL}^{-1}$ ,  $l$ ; pathlength  $\text{cm}$ ;  $M$ ; molecular weight

$$[\theta] \text{ MRW} = \theta / (10 \times cr \times l)$$

$Cr$  (mean residue molar concentration) =  $n \times c$ , where  $n$  is the number of peptide bonds in the protein

# Far UV CD Spectra

Total Signal for a Protein Depends on its  
2<sup>nd</sup>ary Structure



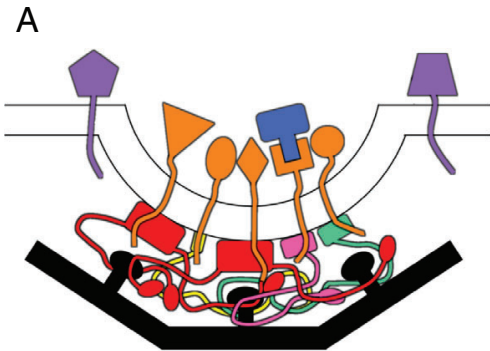
- Notice the progressive change in  $\theta_{222}$  as the amount of helix increases from chymotrypsin to myoglobin

# A real example

---

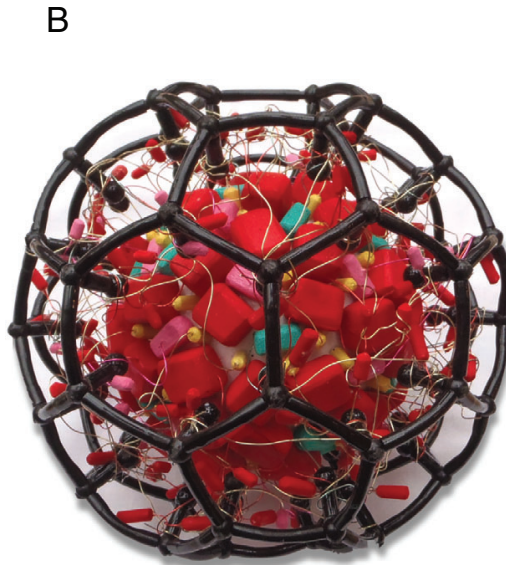
Assembling a puzzle...

# Clathrin mediated endocytosis

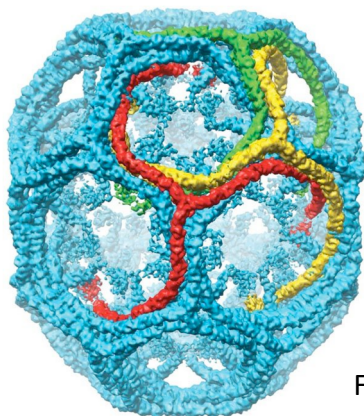


**clathrin**  
**AP (adaptor proteins)**  
**alternative adaptor**  
**transmembrane cargo**  
**luminal cargo**  
**resident proteins**

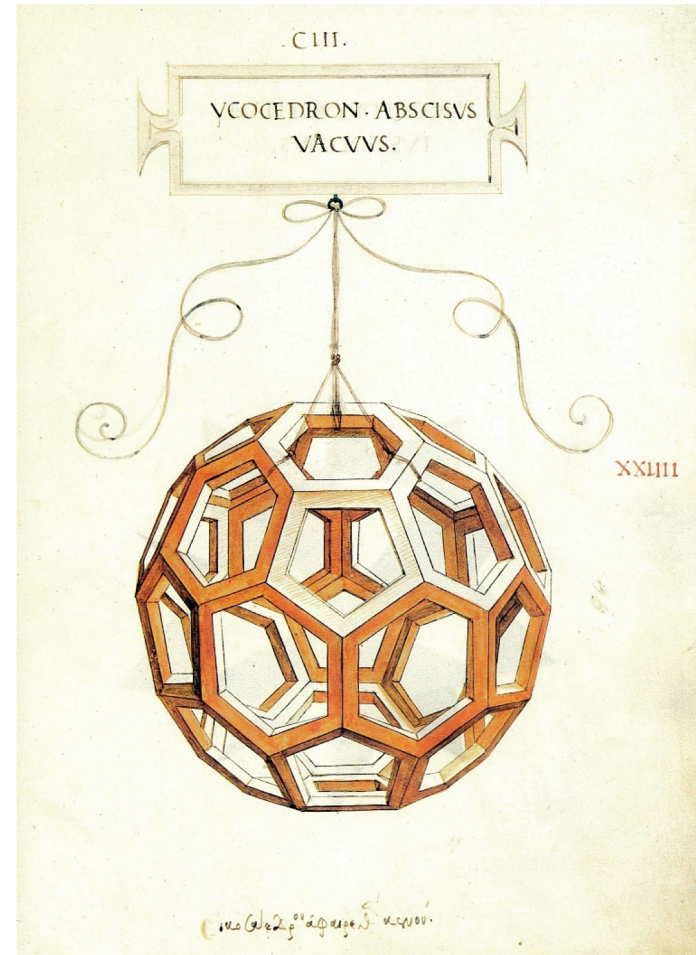
Robinson MS, Review, Traffic 2015



-Model of a Clathrin coated vesicle based on EM and proteomics analysis

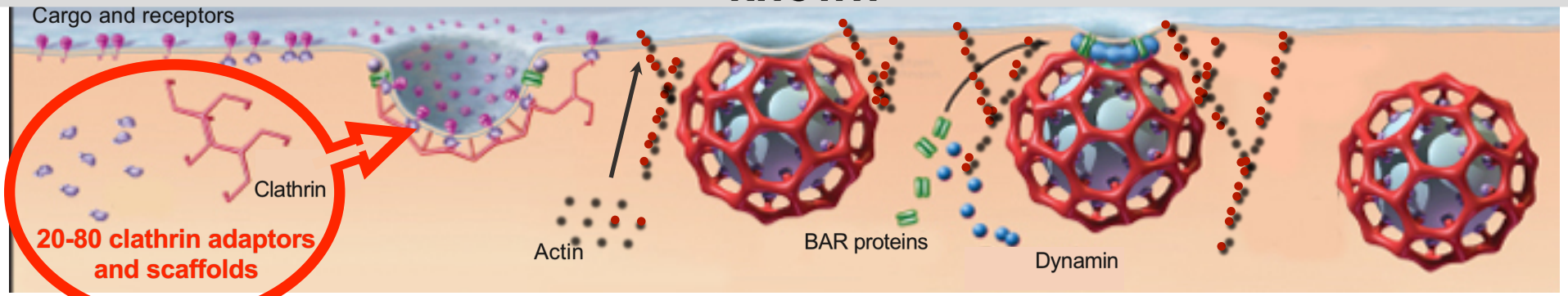


Fotin, et al. Nature. 2004

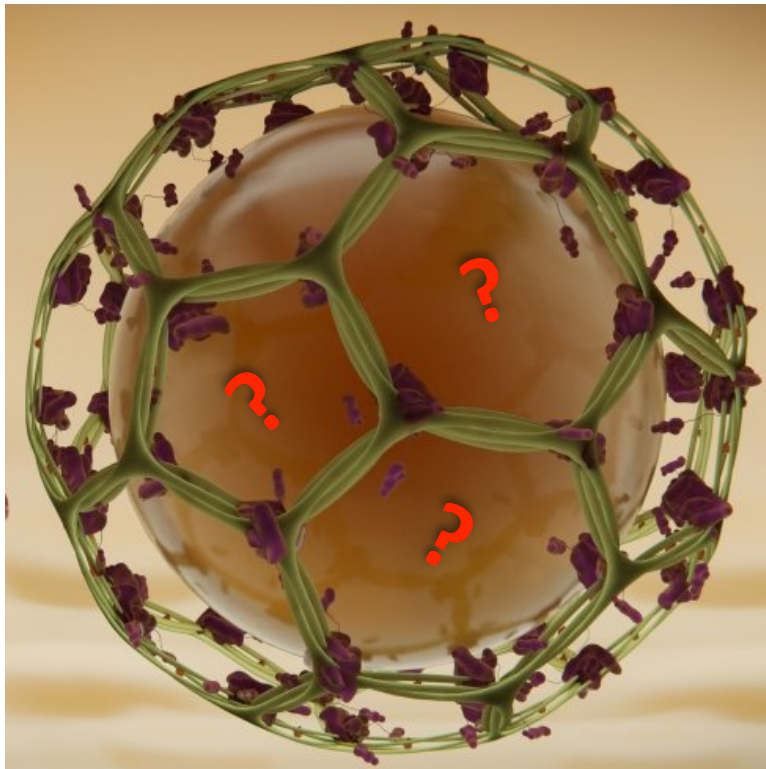


Icosahedron by Leonardo da Vinci (1452-1519)

# Functional organization of the central endocytic coat is not known



adapted from Pollard *et al.*, Cell Biology, 2nd ed., 2007



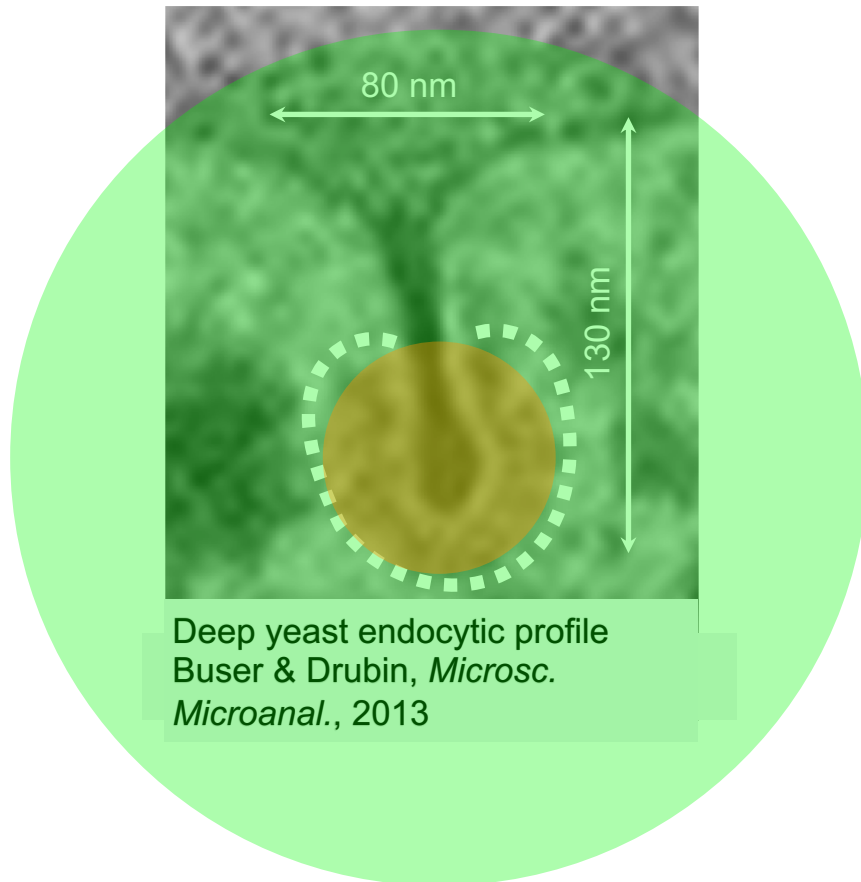
Clathrin-mediated endocytosis poster on Amazon  
(by Stocktrek Images)



model of clathrin-coated vesicle by Prof. Margaret Robinson,  
University of Cambridge

# Mapping of the endocytic coat requires a high spatiotemporal resolution

---



**Methods, we currently use:**

**immunolectron microscopy**

**Idrissi *et al*, 2008, 2012**

**correlative light-electron microscopy**

**Kukulski *et al*, 2012**

**Avinoam *et al*, 2015**

**Sochacki *et al*, 2017**

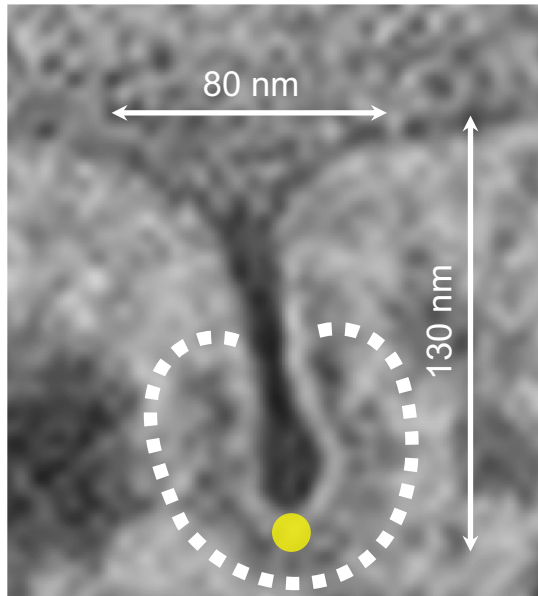
**live-cell imaging of centroid positions**

**Picco *et al*, 2015, 2018**

**single molecule localization  
microscopy**

**Mund *et al*, 2018**

# Mapping of the endocytic coat requires a high spatiotemporal resolution



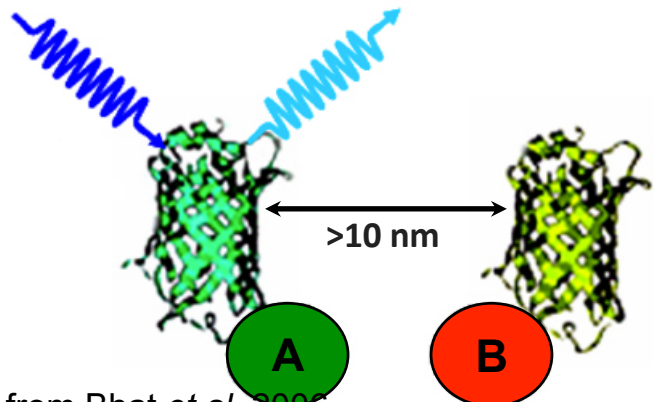
Deep yeast endocytic profile  
Buser & Drubin, *Microsc.  
Microanal.*, 2013

Method, we can use:

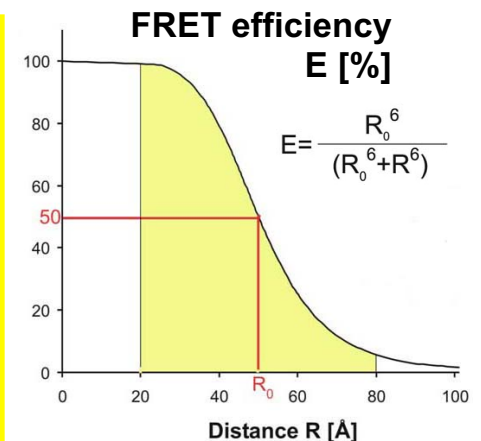
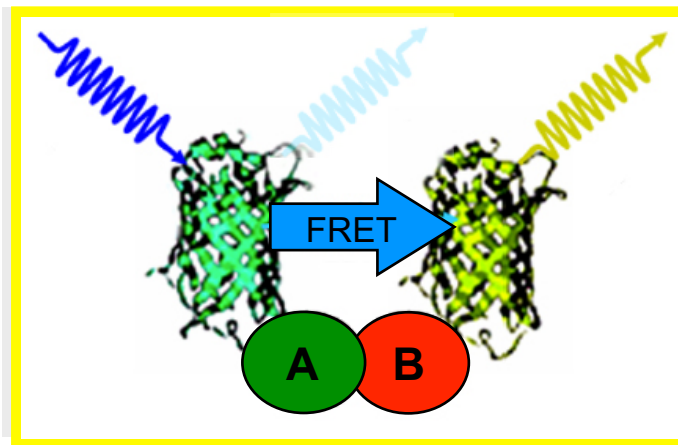
FRET-based protein-protein  
proximity mapping

Förster resonance energy transfer (FRET)  
occurs between fluorophores separated  
by less than  $\sim 10$  nm

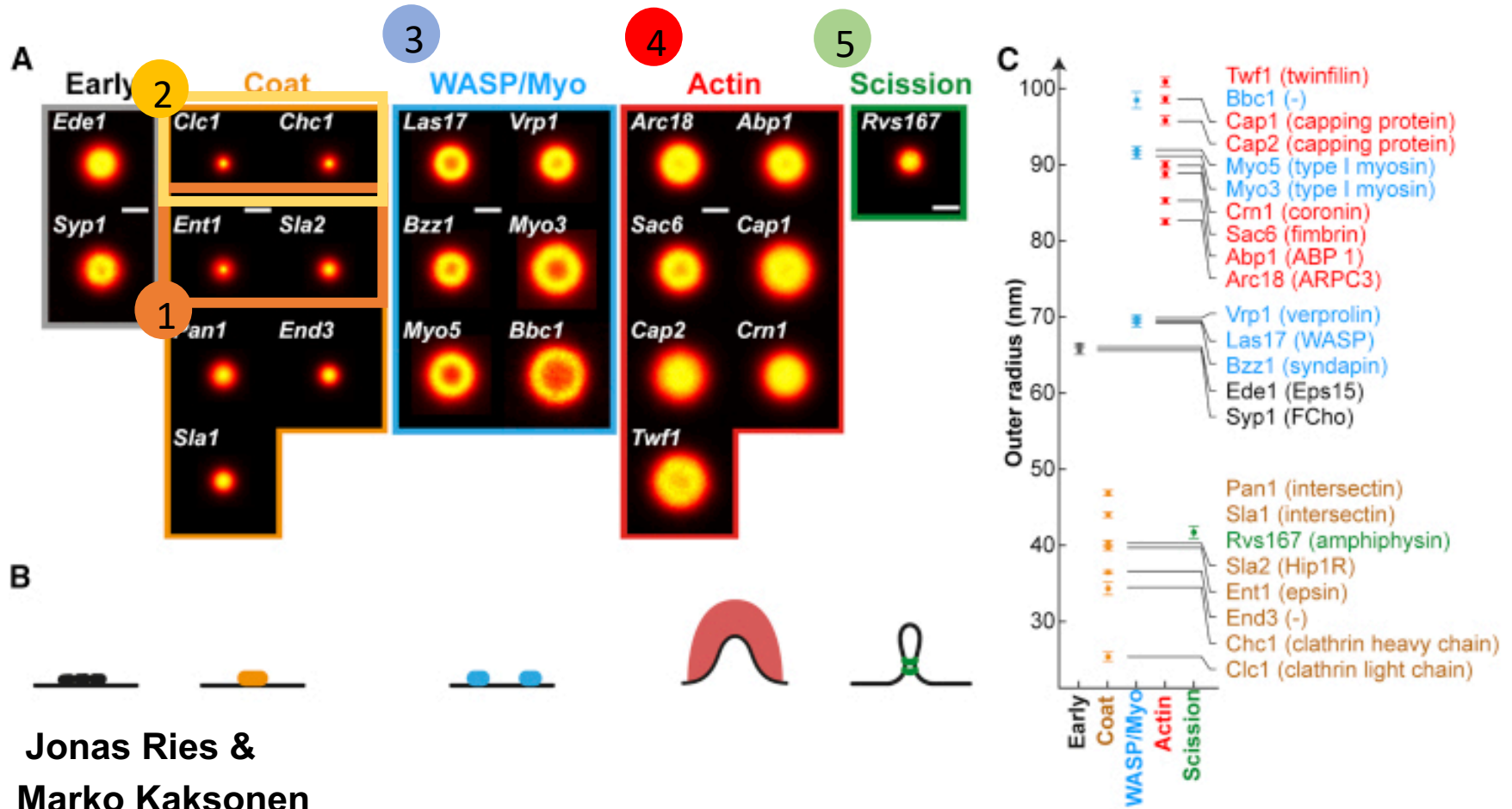
approx. 20 coat-associated proteins  
(each in dozens of copies in semi-  
equimolar ratio) localize  
in a “FRET accessible” area with  
a very good signal/noise ratio!



from Bhat *et al*, 2006



# Superresolution microscopy on the endocytic site

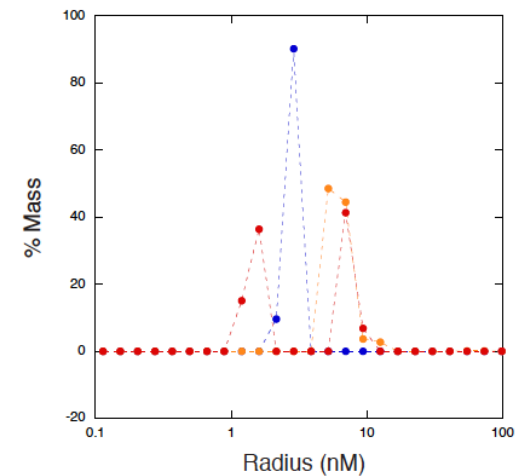
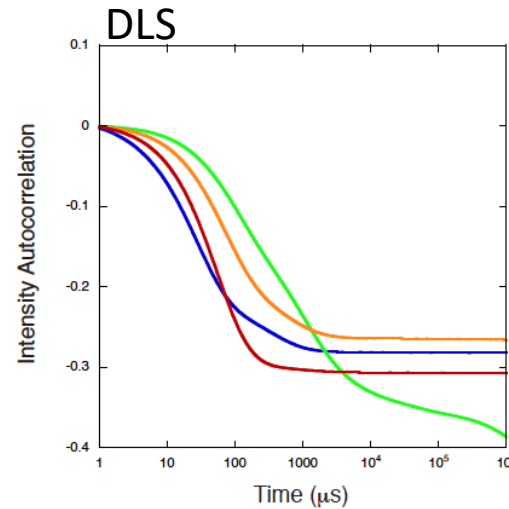
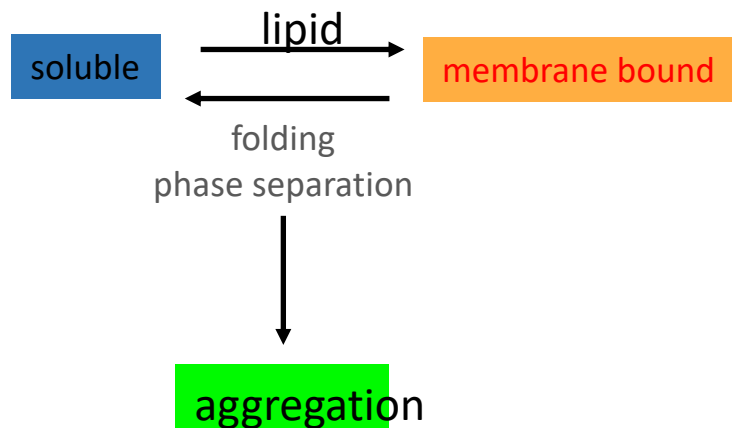
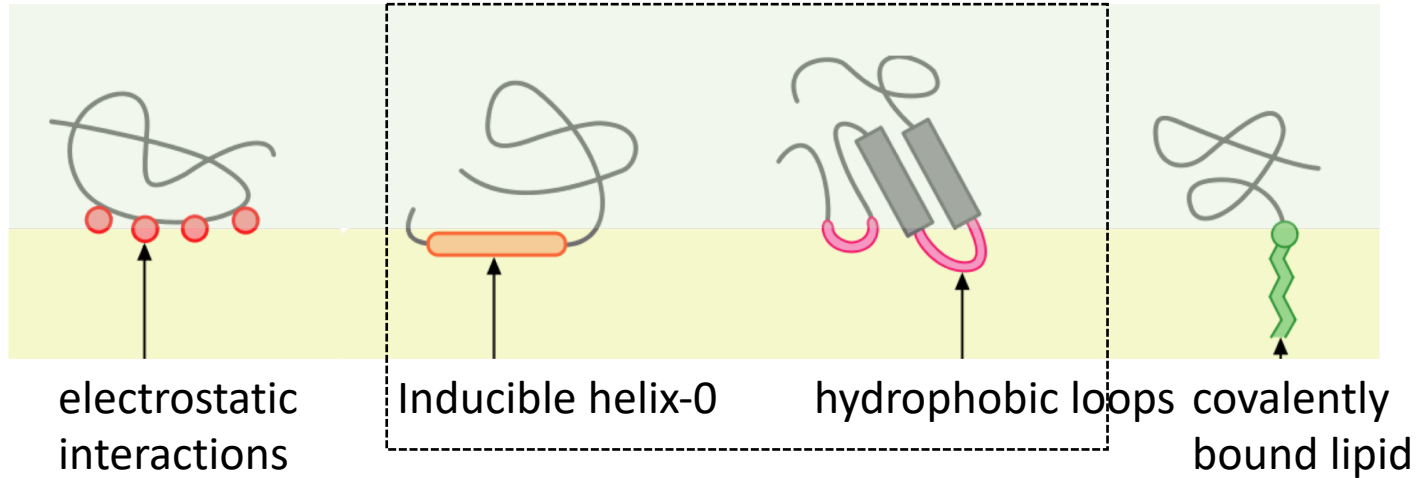


Jonas Ries &  
Marko Kaksonen

# ENTH and ANTH are membrane targeting domains

(Lipid Clamps) PIP2

amphitropic domains

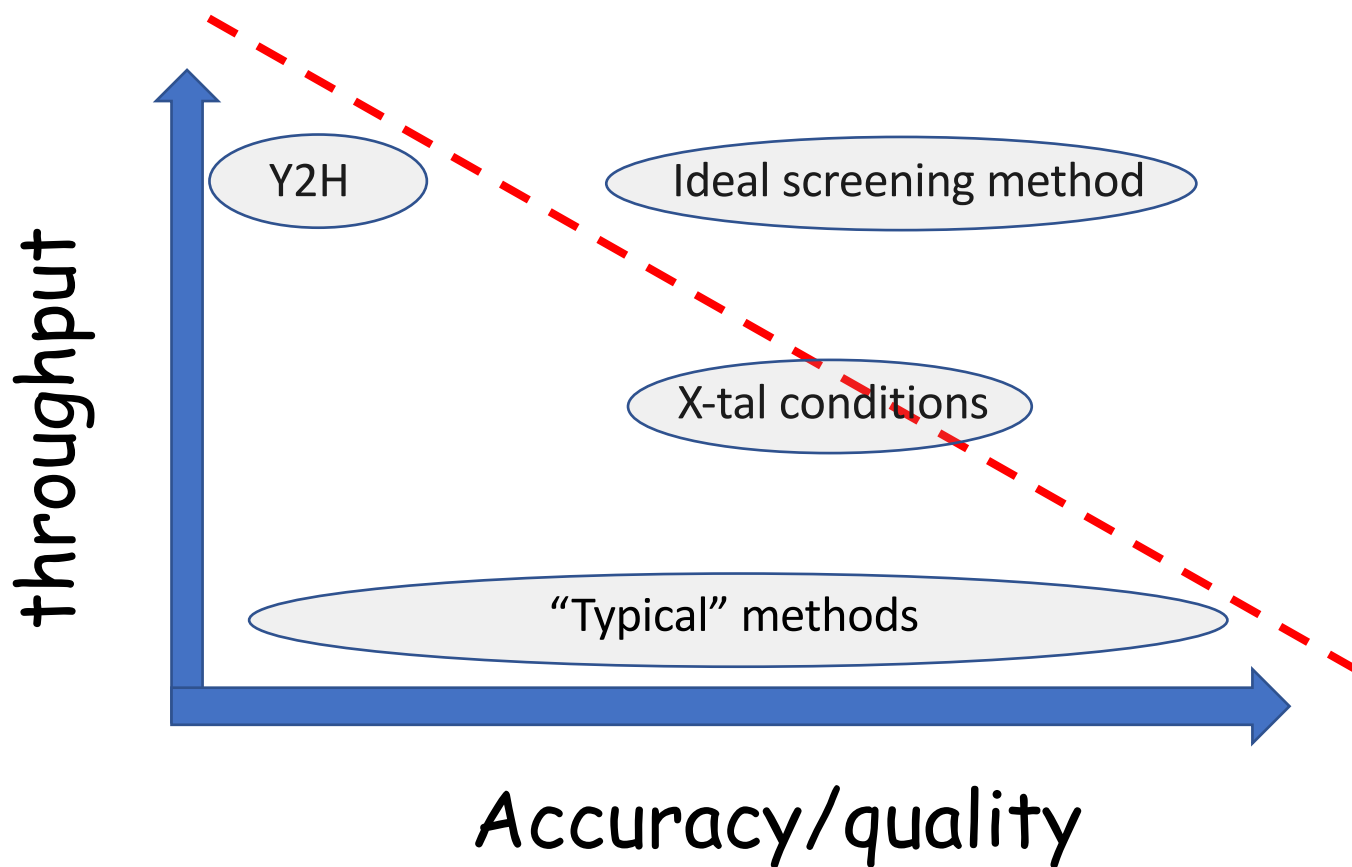


# Protein-Protein interaction

---

Do these proteins form a complex?

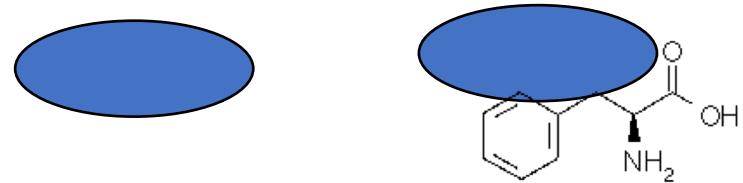
# Screening



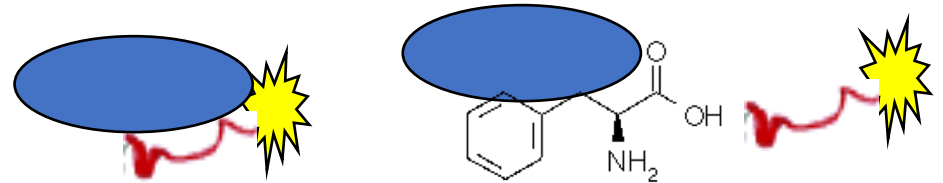
Small molecules  
Binding  
X-tal conditions  
Stability  
Grow conditions  
Inhibitors  
Expression  
Etc etc etc

# Screening for binding

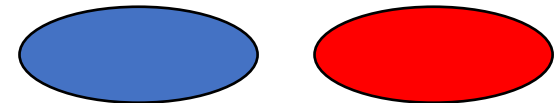
Analytical centrifugation



Fluorescence anisotropy - competition

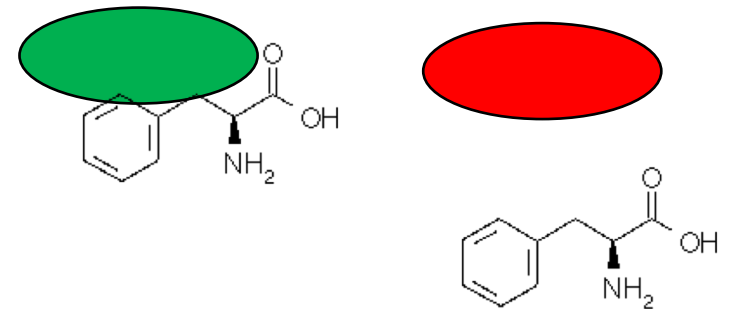


Stability measurements/Mass-action law



DSC

Differential Scanning Fluorimetry  
(DSF, ThermoFluor, SYPRO Orange, qPCR)

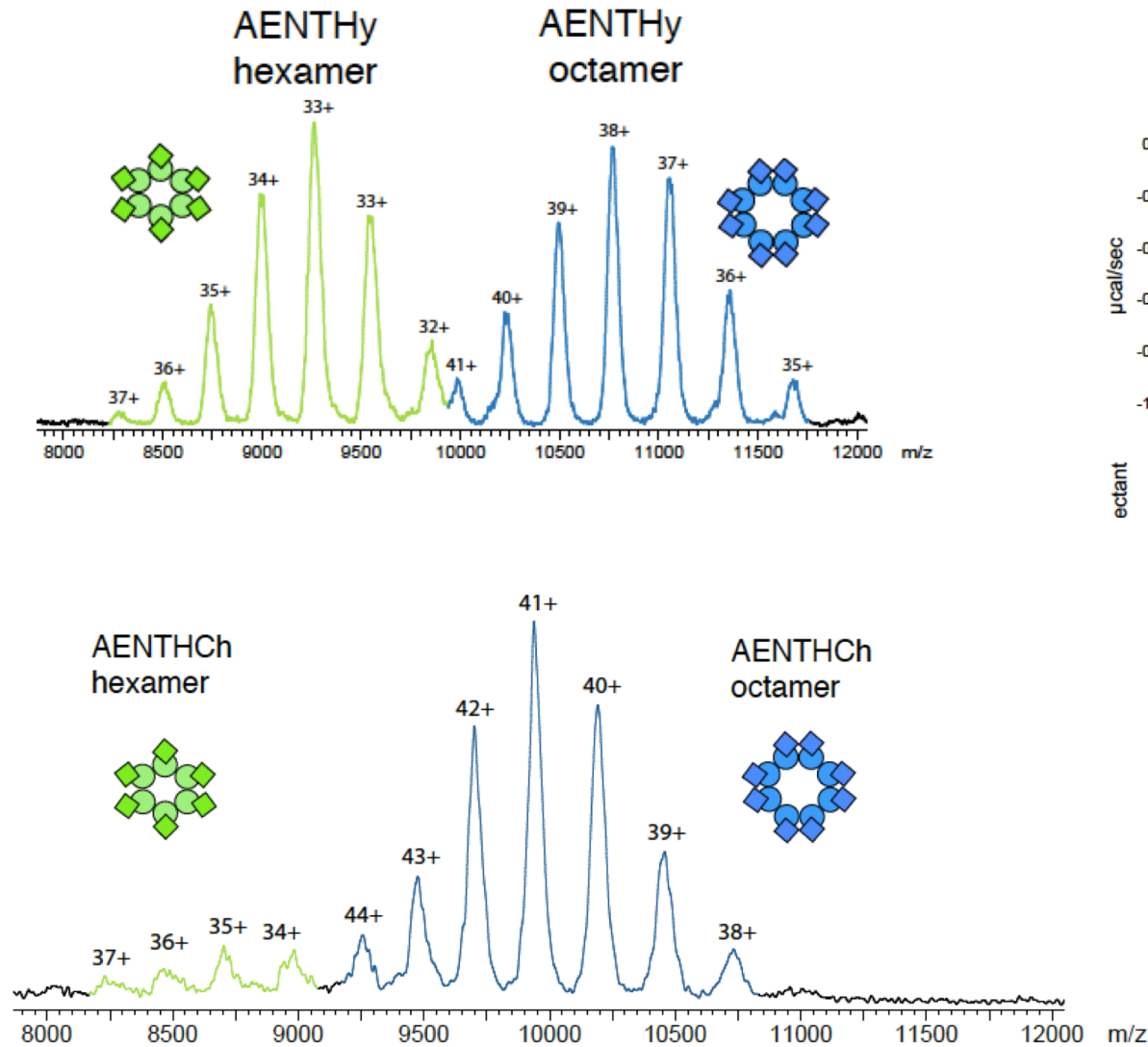


Temperature

# Summary

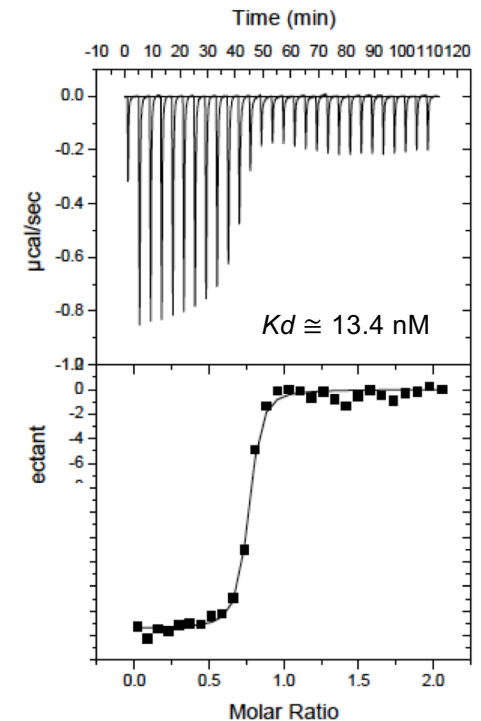
- Balance between quality and throughput
- Established system
  - Soluble
  - Stable
  - Characterised
- Reliable protein production (>1g)
- Model ligand
- Source of potential ligands to test
- Ways of designing next diversity set

# An Hexameric and an Octameric AENTH



**NMS**

**ITC**



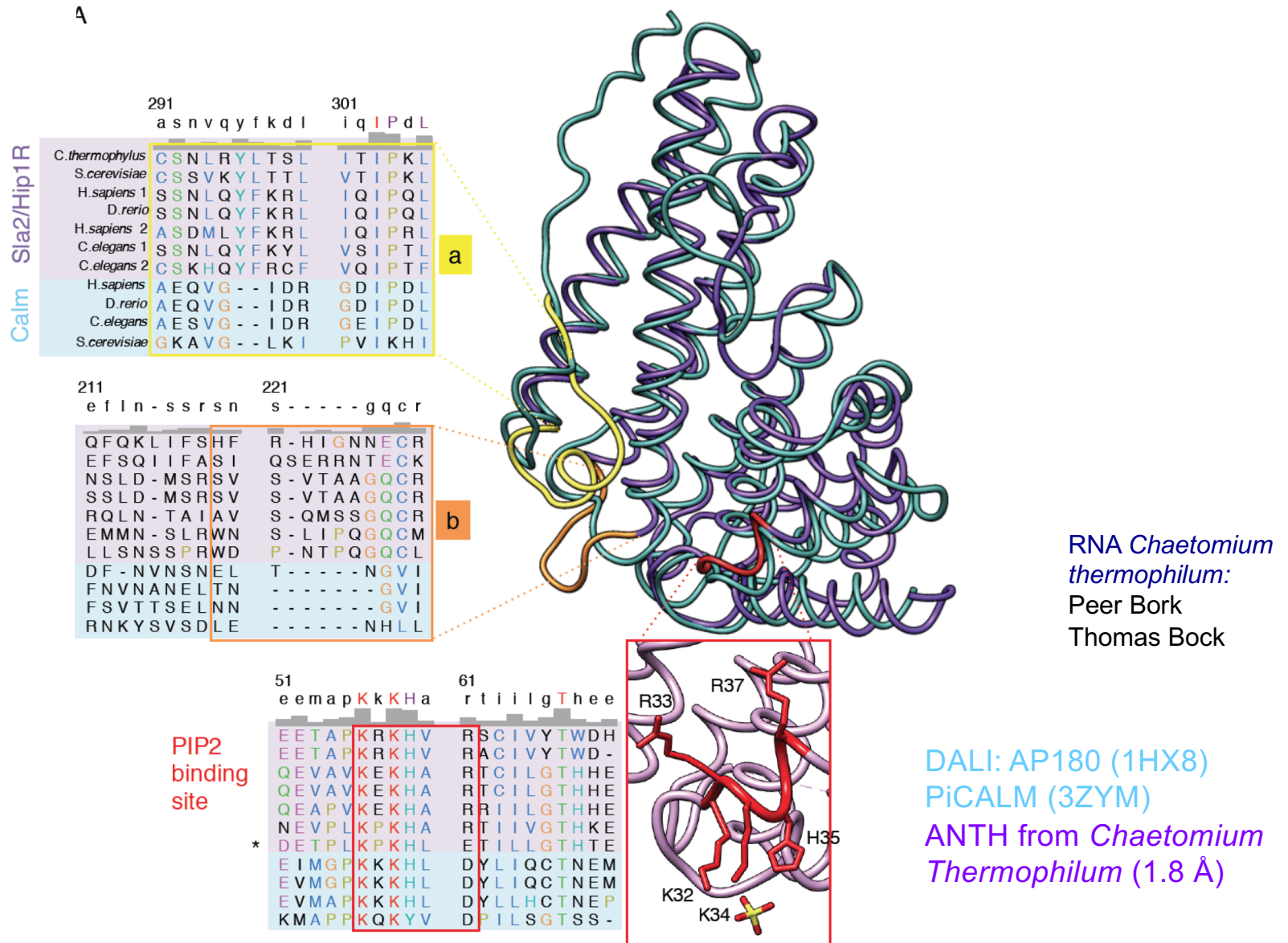
**SAXS**

**Observed  $M_r$  (Da) [from  $I(0)$ ]**  
342 KDa  $\pm$  30 KDa

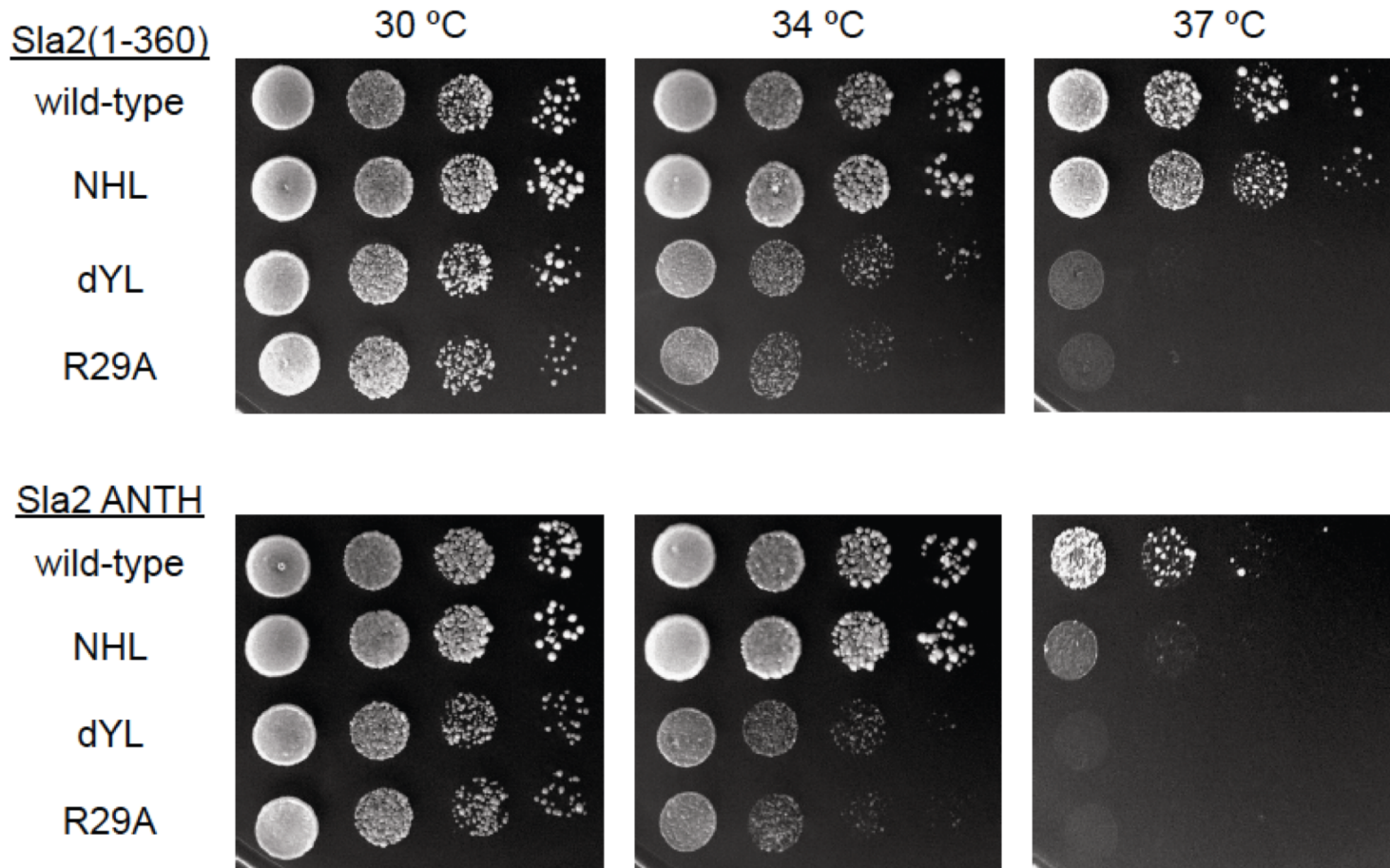
**Expected  $M_r$  Hexamer:** 313 KDa  
**Expected  $M_r$  Octamer:** 417 KDa  
**Expected Average:** 365 KDa



# Structural Differences between Calm and ANTH subfamilies

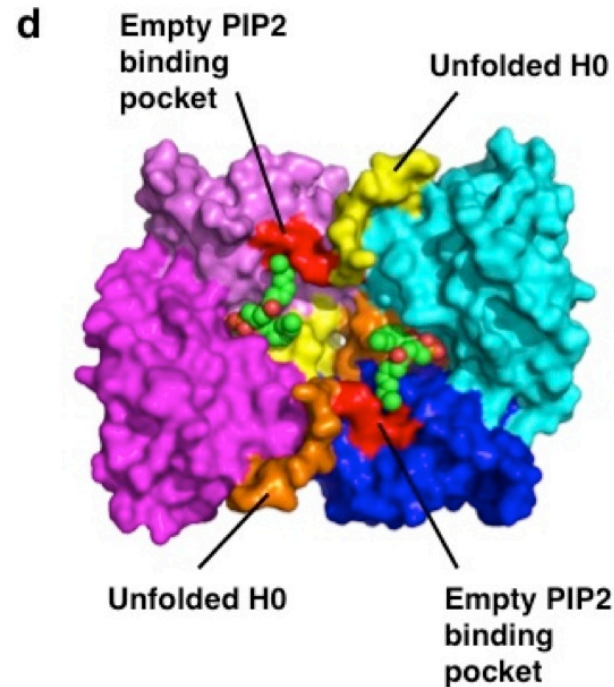
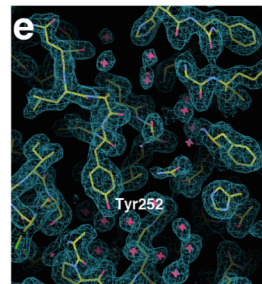
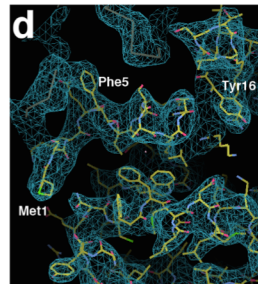
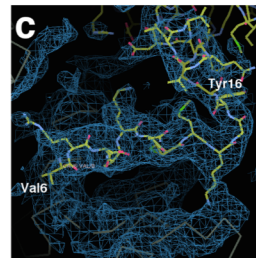
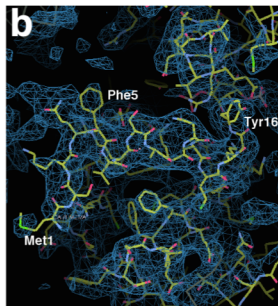
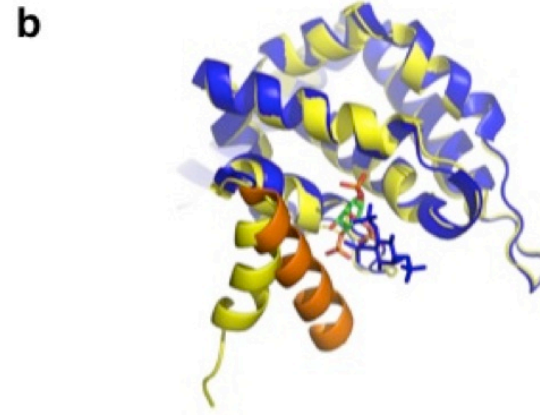
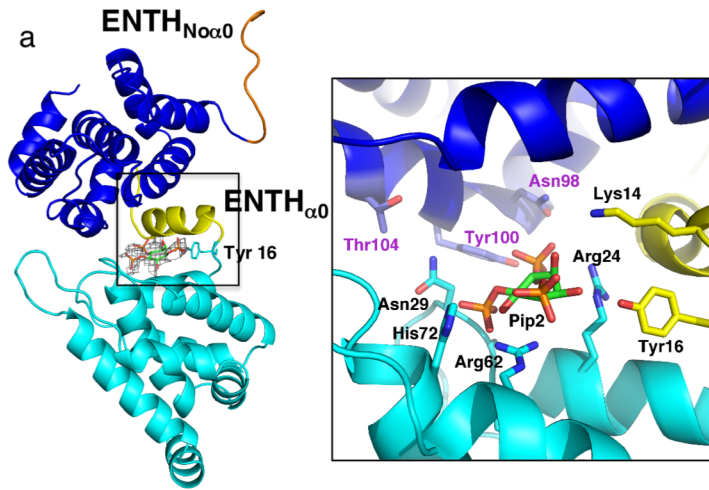


# Structural Differences between Calm and ANTH subfamilies



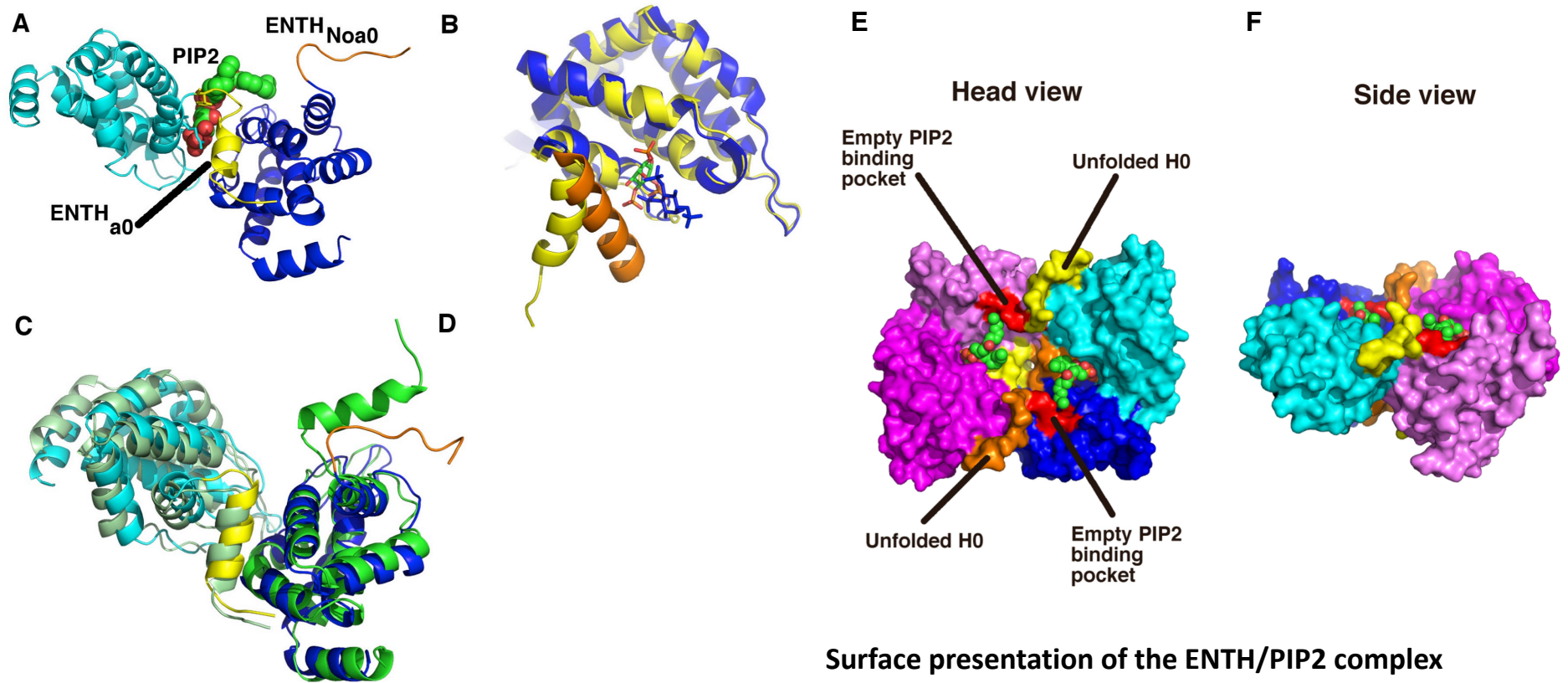
-Growth defects of Sla2  $\Delta$ YL and  $\Delta$ NHL mutant strains. Ten-fold serial dilutions of *s/a2D* strains expressing indicated proteins were incubated on SC-Ura plates for 1.5–2 days at 30C, 35C, and 37C.

# Crystal structure of the ENTH2/PIP2 complex reveals an allosteric-binding mechanism



# Epsin forms assemblies through phospholipid interfaces

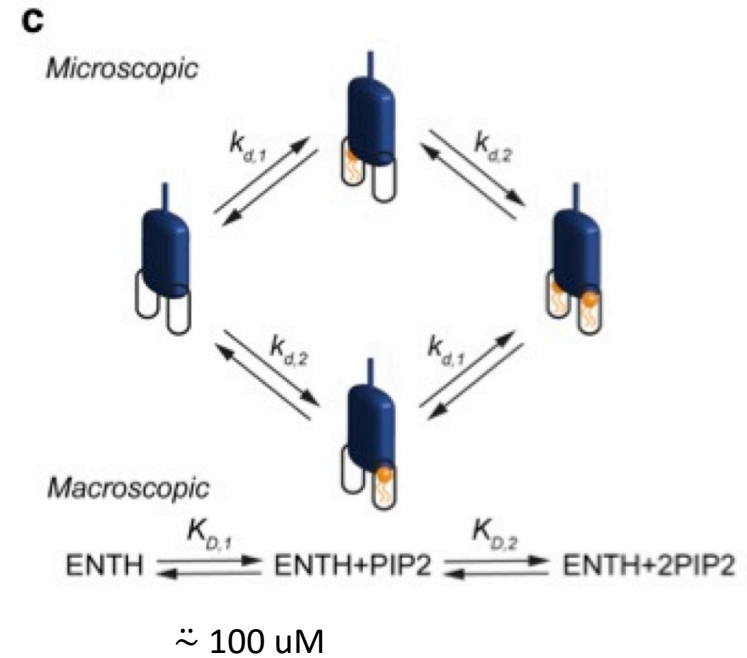
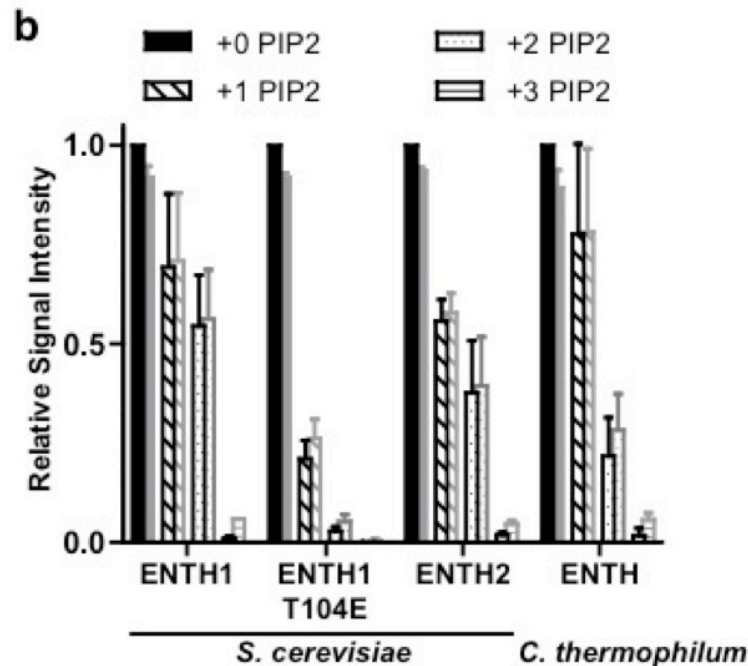
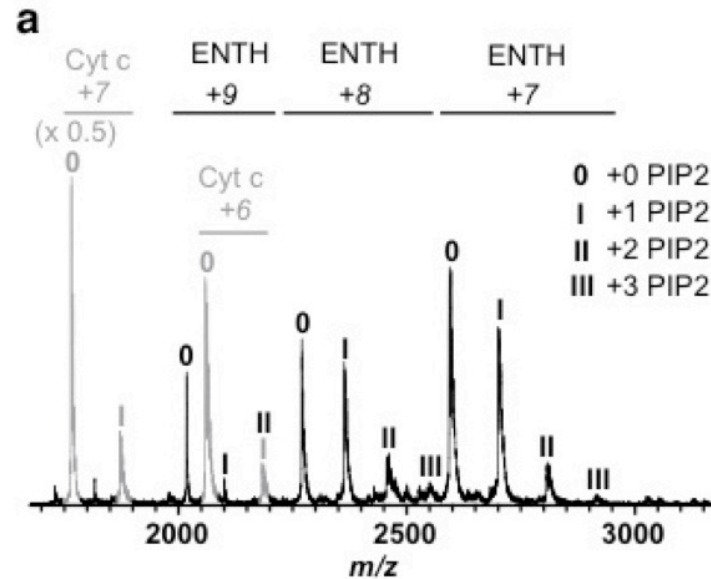
Crystal structure of Epsin ENTH bound to PIP2



Surface presentation of the ENTH/PIP2 complex showing a tetrameric assembly

- Two building blocks in cyan/blue and magenta/violet
- Tyr 16, Arg 24, Arg 62 and His 72 form the empty PIP2 binding pocket

# Cooperative binding of PIP2 to the ENTH domain of epsin

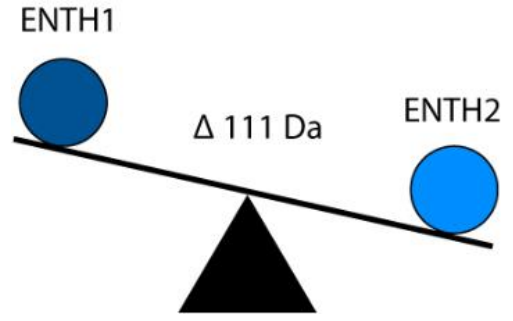
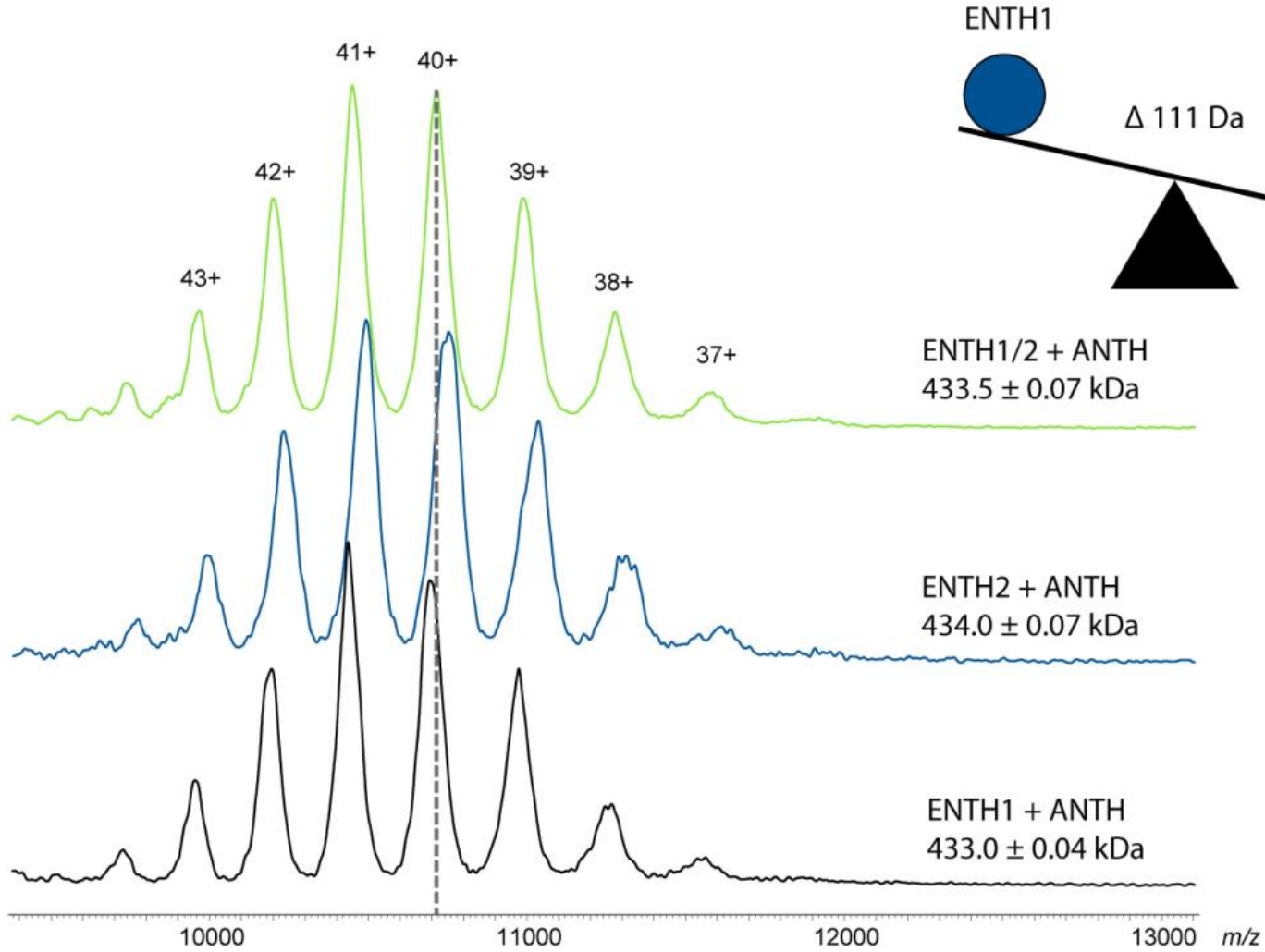
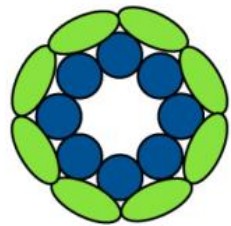
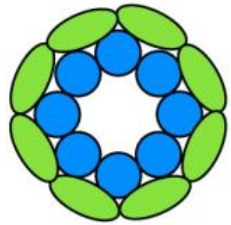
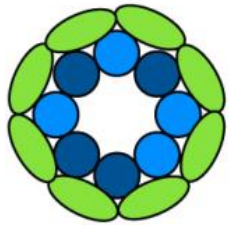


- Relative peak intensities were used to determine the ratio of lipid-bound to non-bound
- Cooperativity of the two binding sites was assessed by reviewing the mathematical relation:

$$K_{D,1} = \frac{k_{d,1} \times k_{d,2}}{k_{d,1} + k_{d,2}}$$

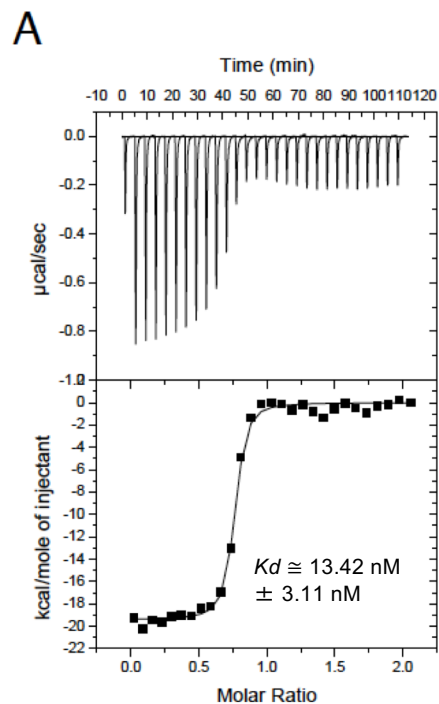
$$K_{D,2} = k_{d,1} + k_{d,2}$$

# Complexes with ENTH1 and ENTH2

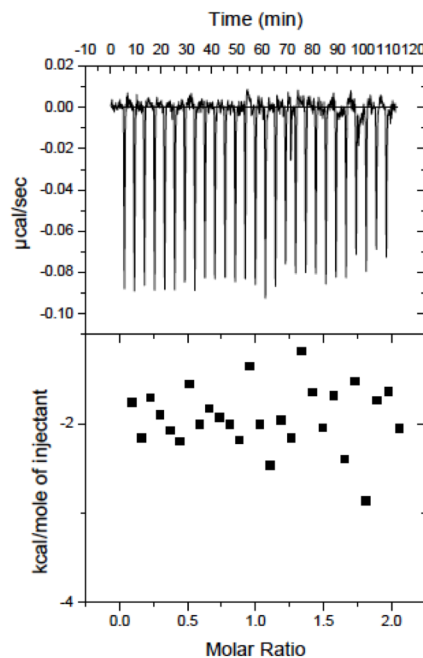


# PIP2 availability as the regulatory mechanism for AENTH assembly

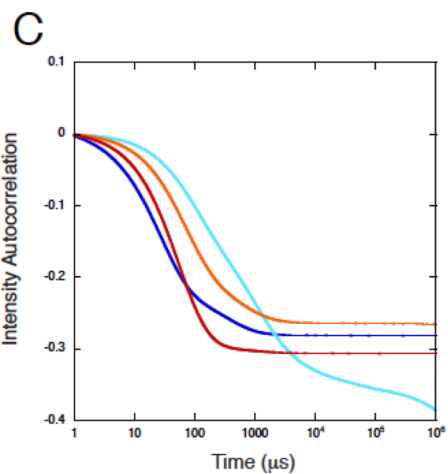
ITC



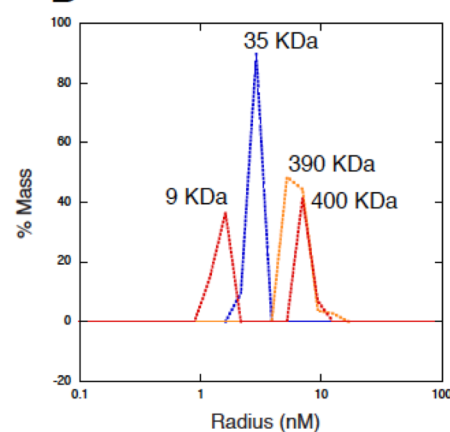
**B**



DLS

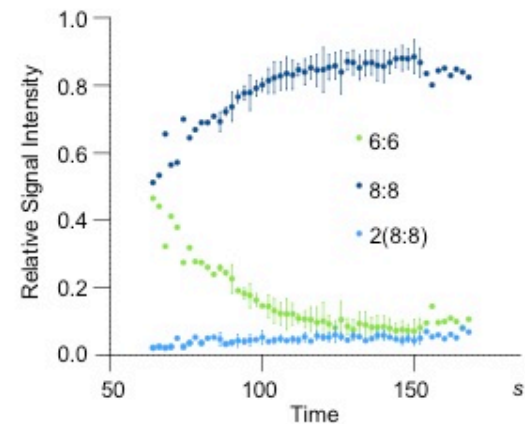
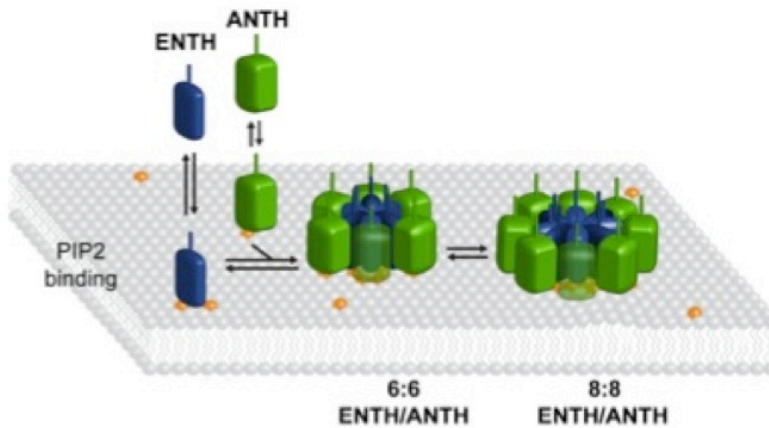
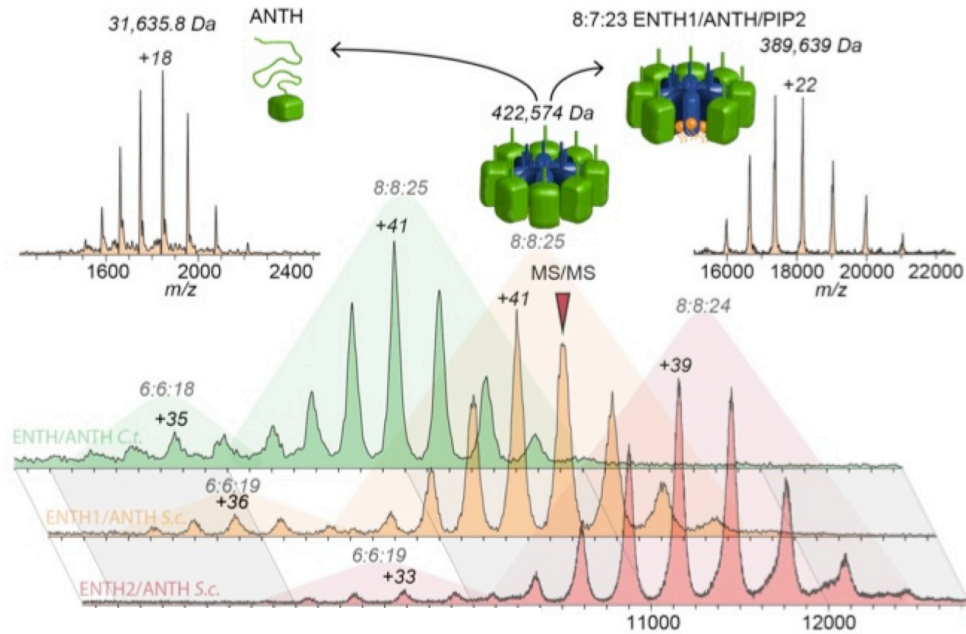


**D**



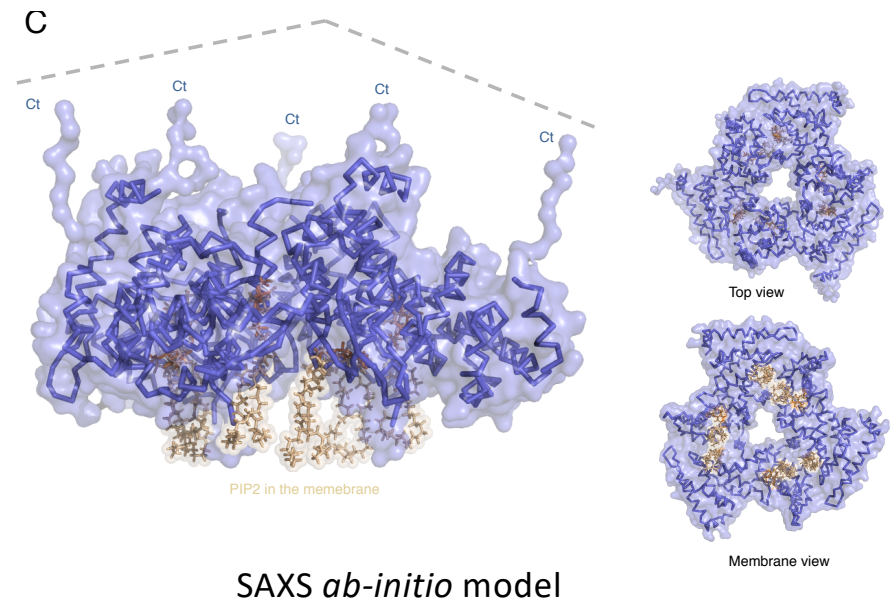
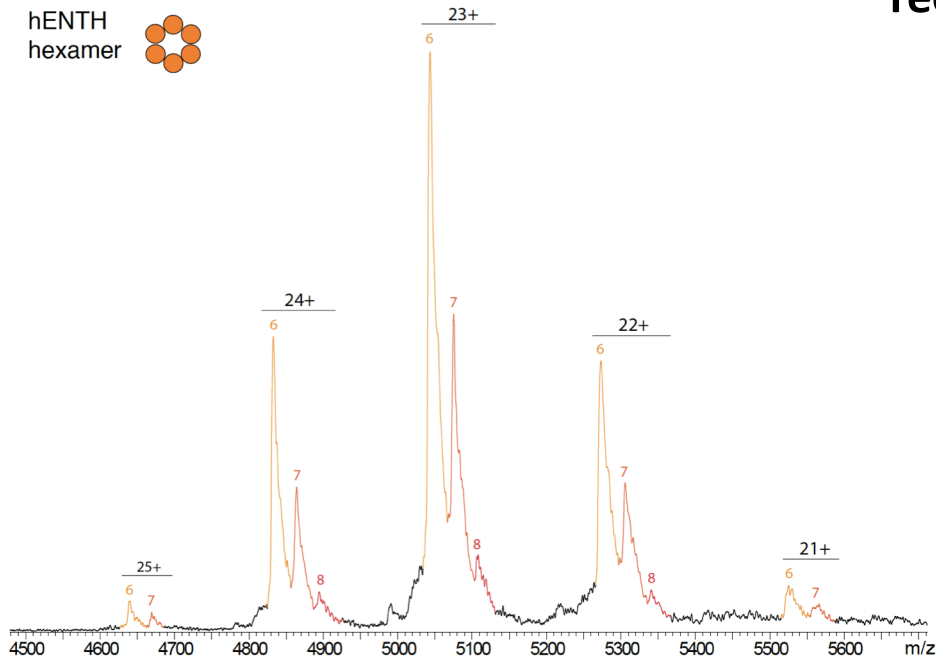
[PIP2]= 0  $\mu\text{M}$ , blue; 80  $\mu\text{M}$ , light-blue; 200  $\mu\text{M}$ , orange and 400  $\mu\text{M}$ , red

# Ordered assembly formation of fungal ENTH and Sla2 ANTH



# The human ENTH core

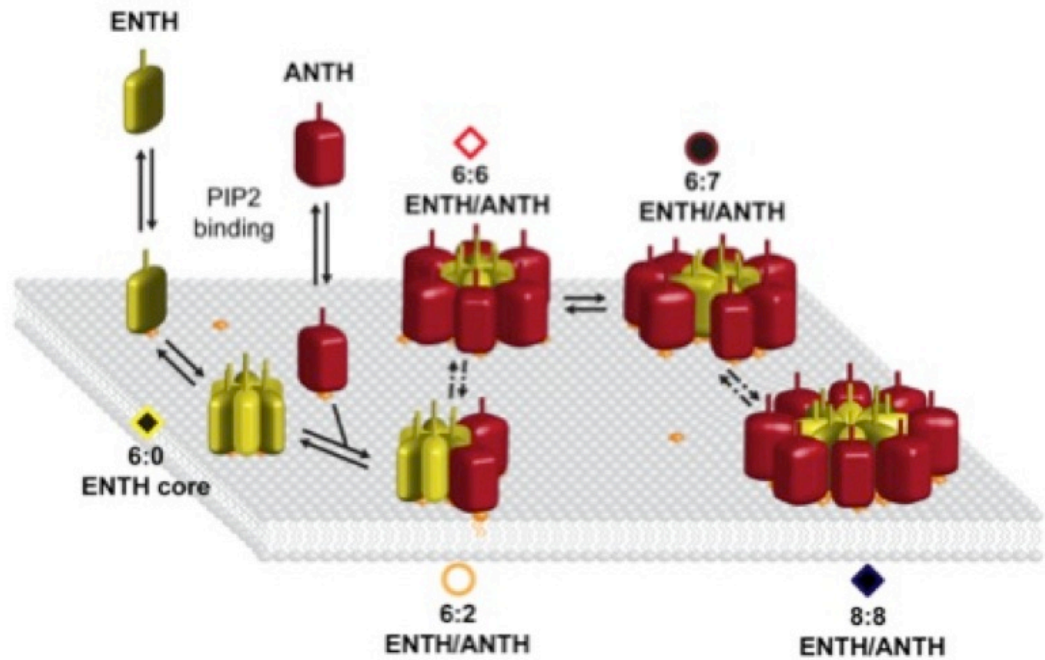
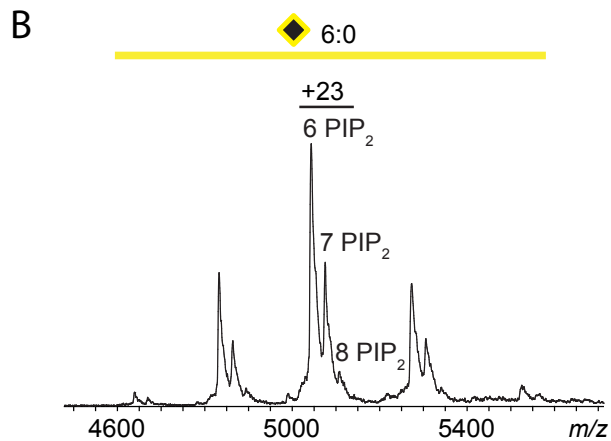
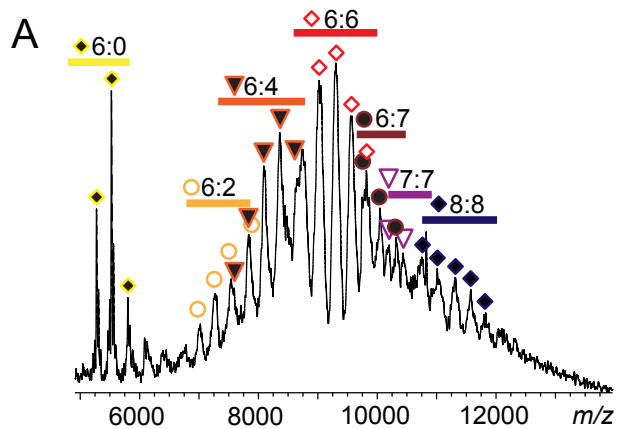
- this could explain the **epsin dependent Hip1R recruitment** observed *in vivo*...



- Is this ENTH core a precursor for further AENTH oligomerization?

# The mechanism of assembly

Biophysics, Crystallography, SAXS and NMS



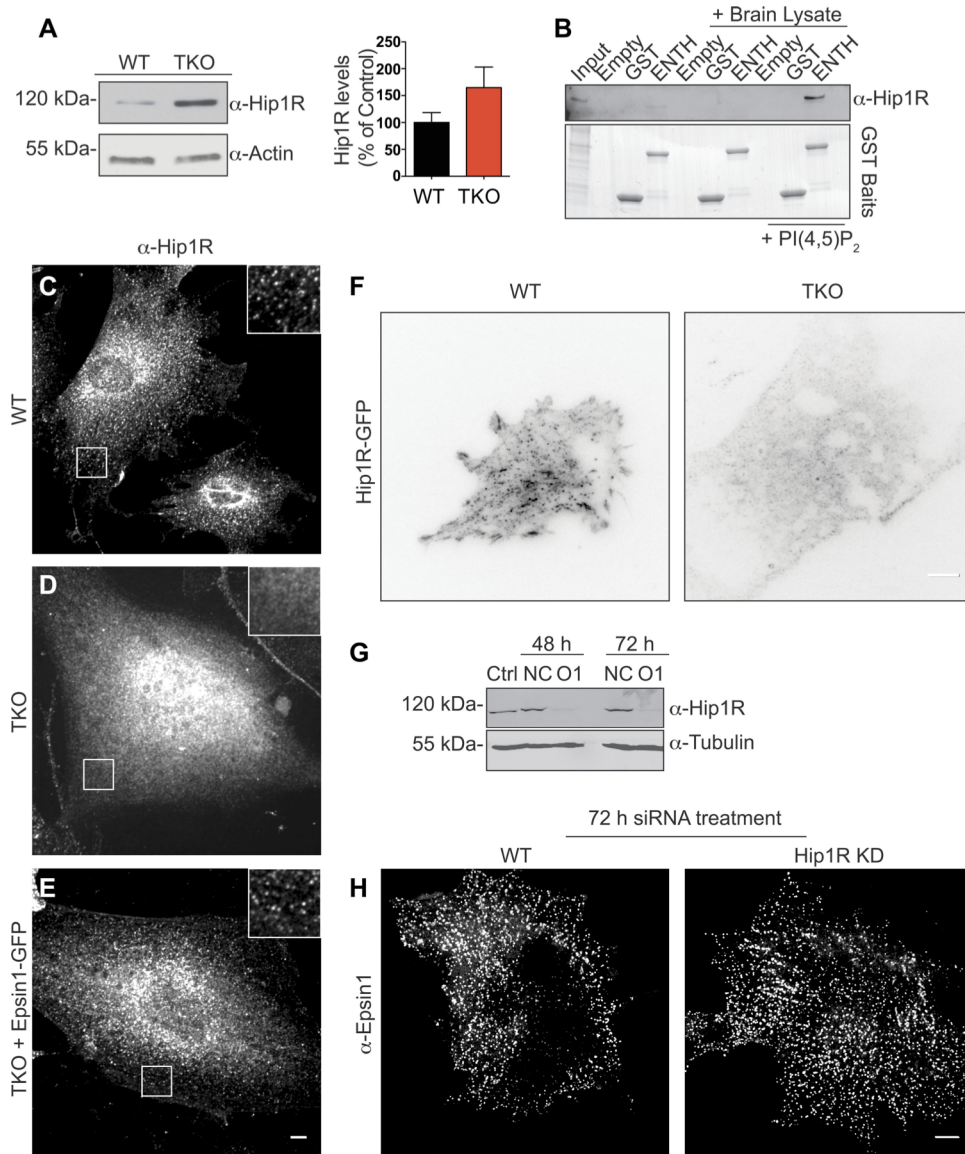


# Question

---

- Is this complex **evolutionary conserved** as a common feature crucial for the clathrin-dependent endocytic path, **or** was it selected as a mechanism occurring **only in yeast?**

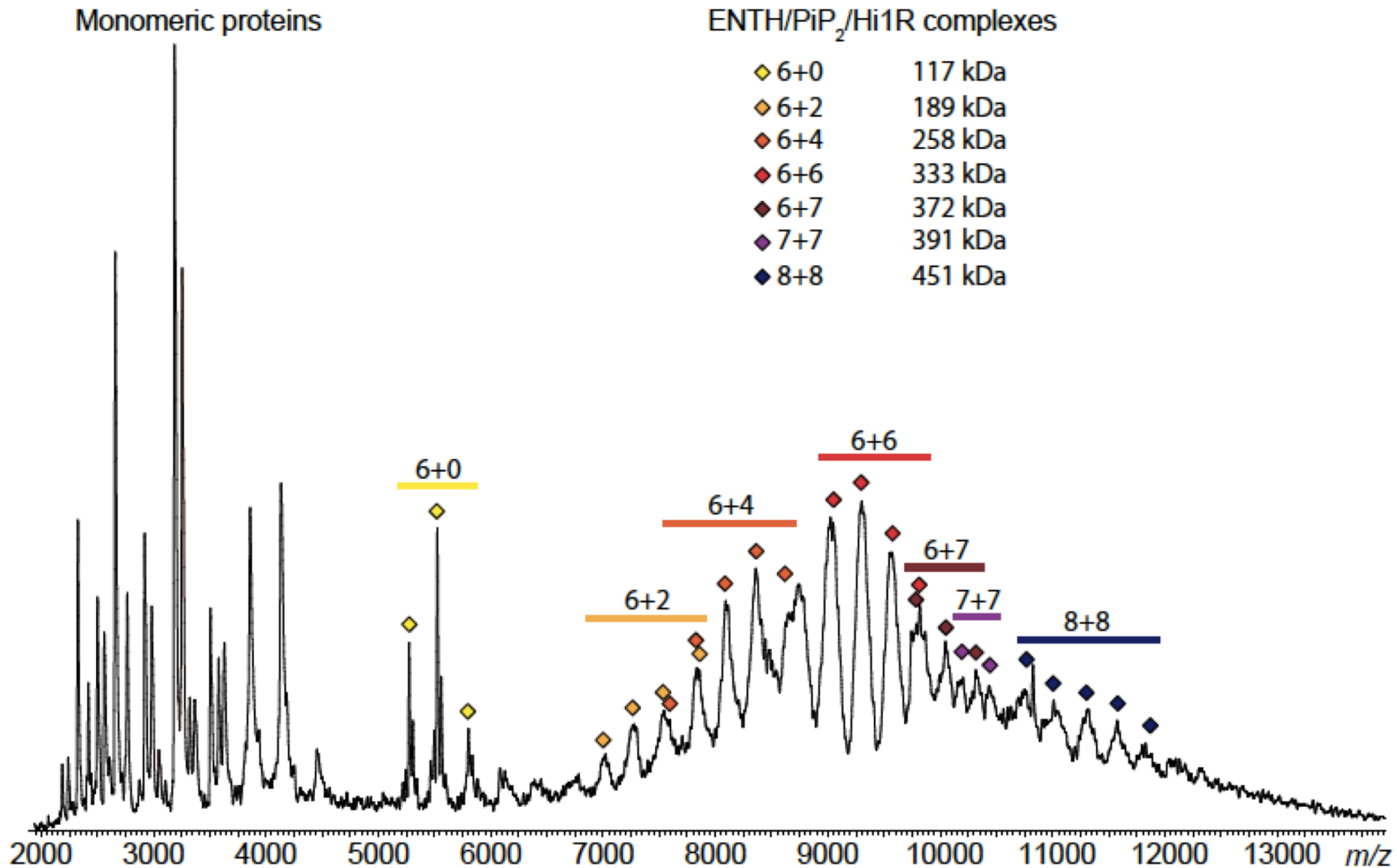
# The typical clathrin-coated pit-like punctate localization



Pull-down experiments from rat brain homogenate, using ENTH domain of epsin 1 as bait revealed an enrichment of Hip1R in the affinity-purified material in the sample also containing PIP<sub>2</sub>

H) siRNA-mediated knockdown of Hip1R does not affect epsin localization in HeLa cells as shown by epsin immunofluorescence.

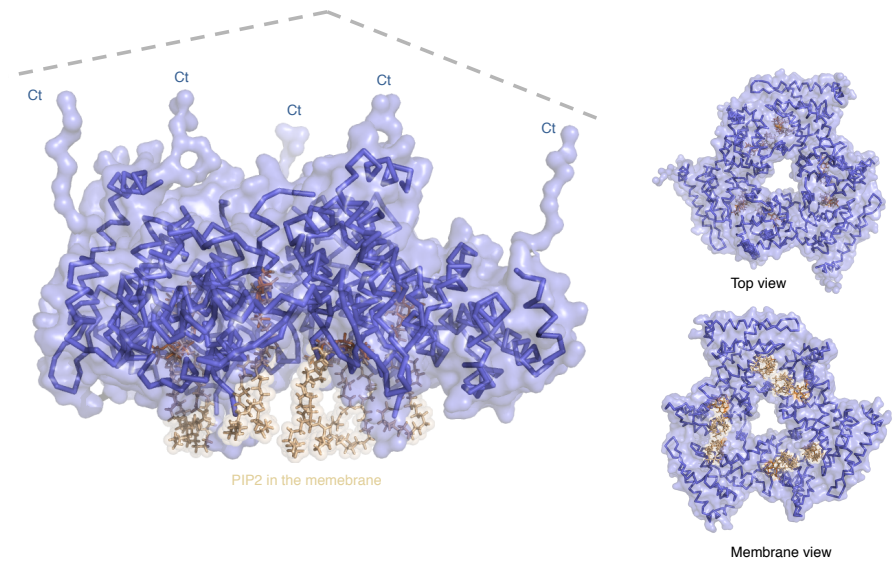
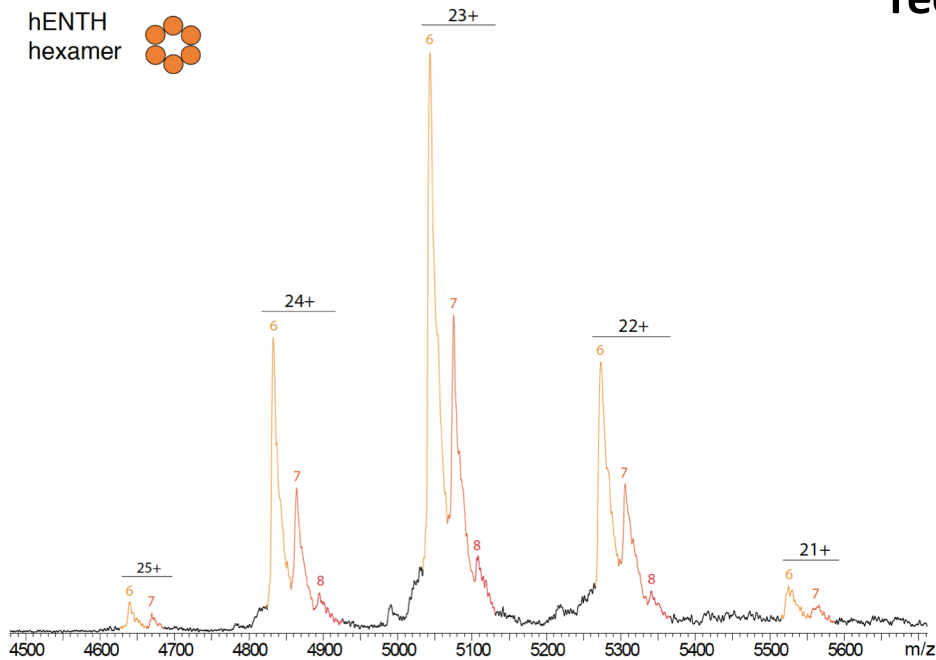
# The AENTH human complex



# The human ENTH core

- this could explain the **epsin dependent Hip1R recruitment** observed *in vivo*...

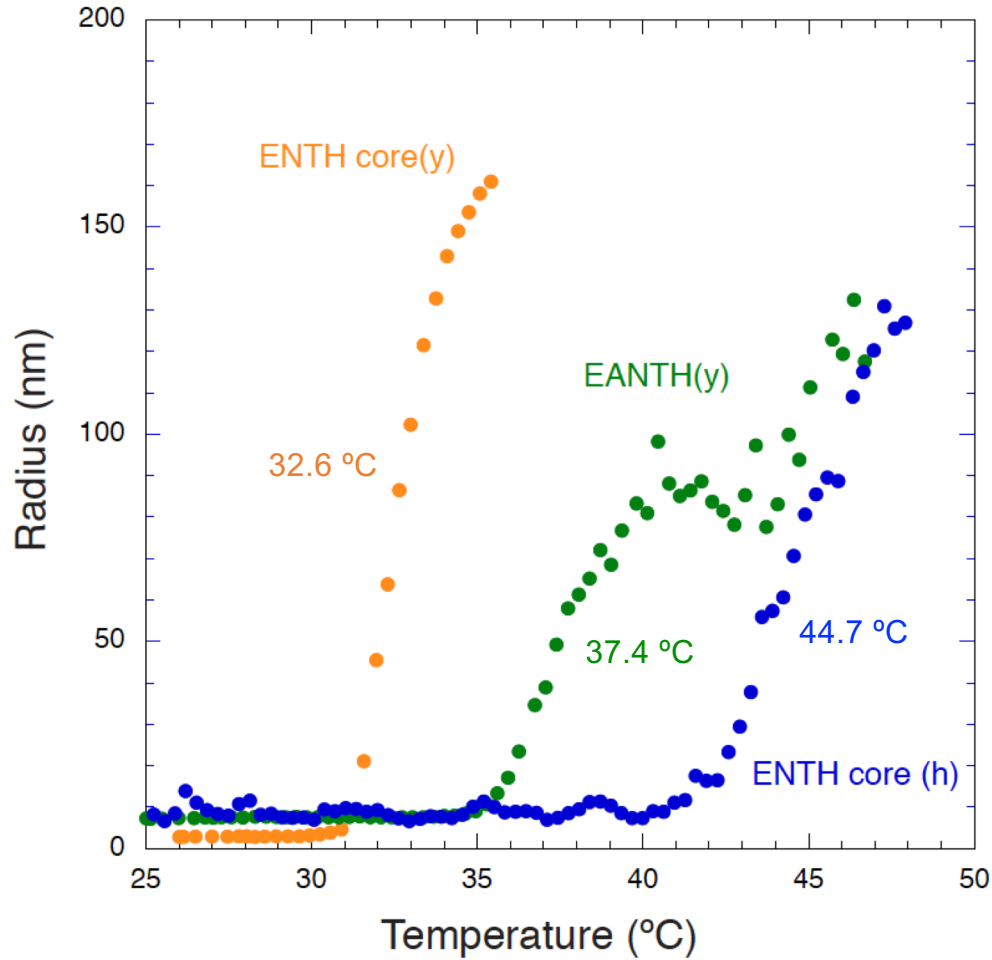
hENTH hexamer



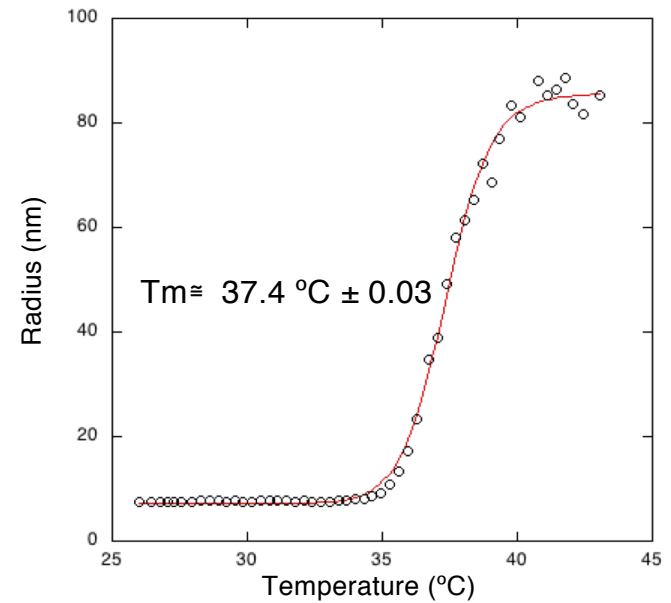
SAXS *ab-initio* model

- Is this ENTH core a precursor for further AENTH oligomerization?

# human ENTH core is stable on its own

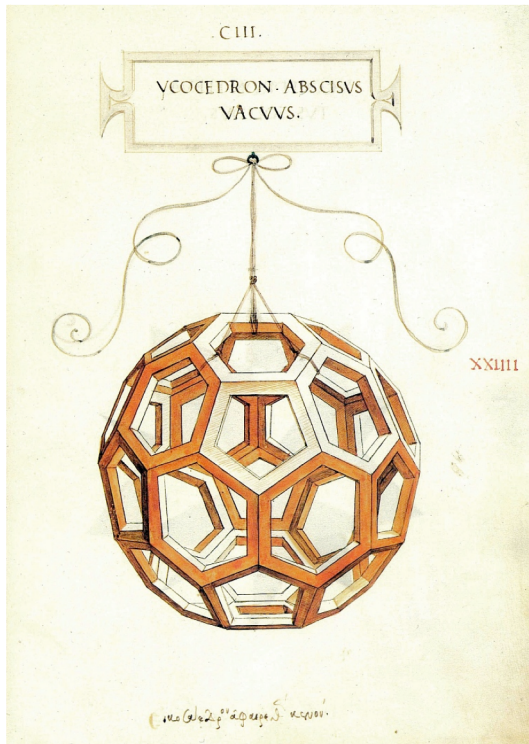


The AENTH complex is more stable than the ENTH-PIP2

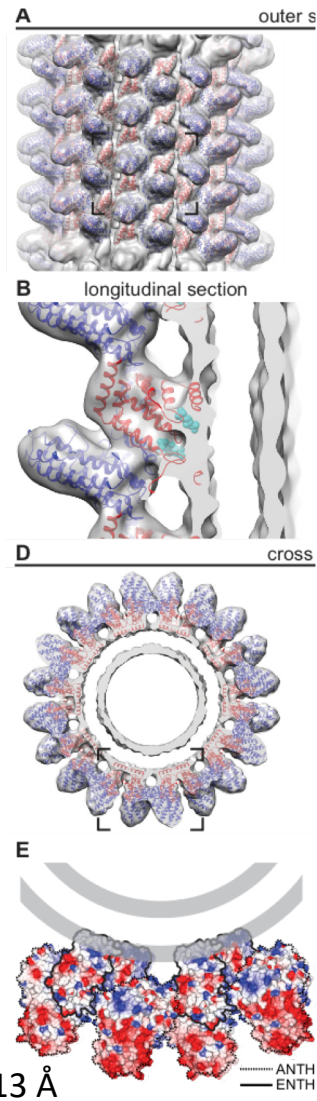


Increase in Rh as a function of temperature monitored by DLS

# The puzzle?

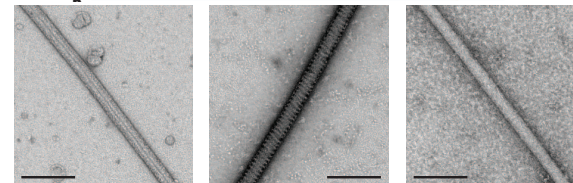
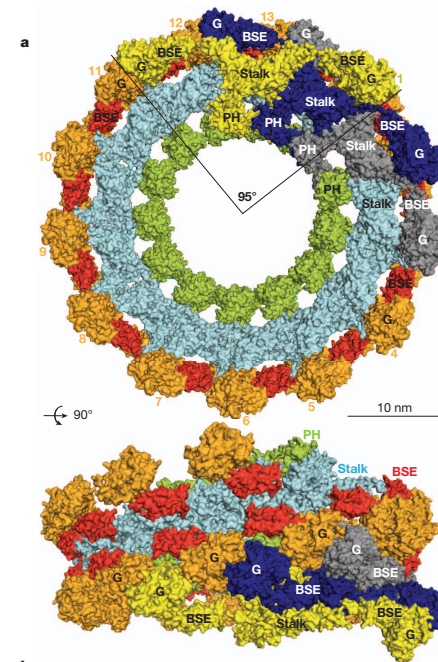


CLC by Leonardo da Vinci?

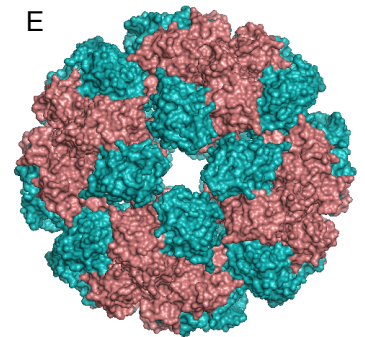
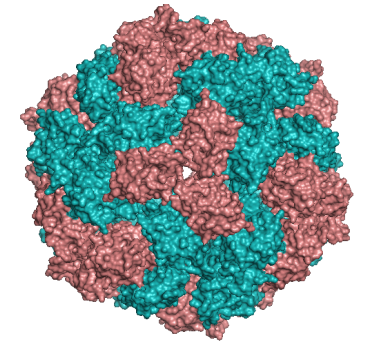


Skruczny *et al.* Dev. Cell, 2015

assembly in GUVs



Ford *et al.* Nature 2011  
Faelber *et al.* Nature 2011



3.8 Å

Our ENTH2 + PIP2  
F432 symmetry

probably not...

# cryo-EM on GUVs with PIP2

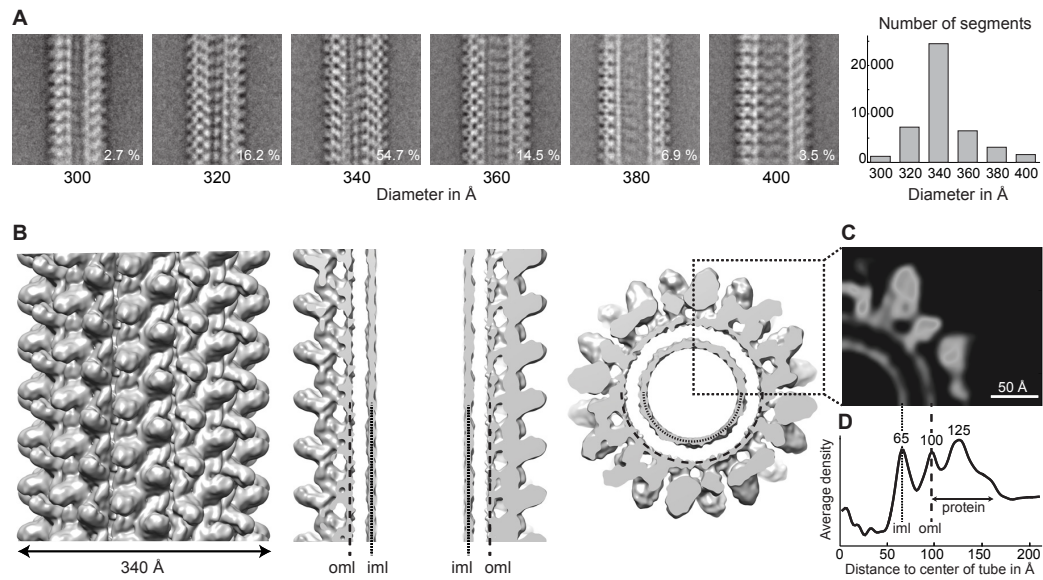


Figure 3

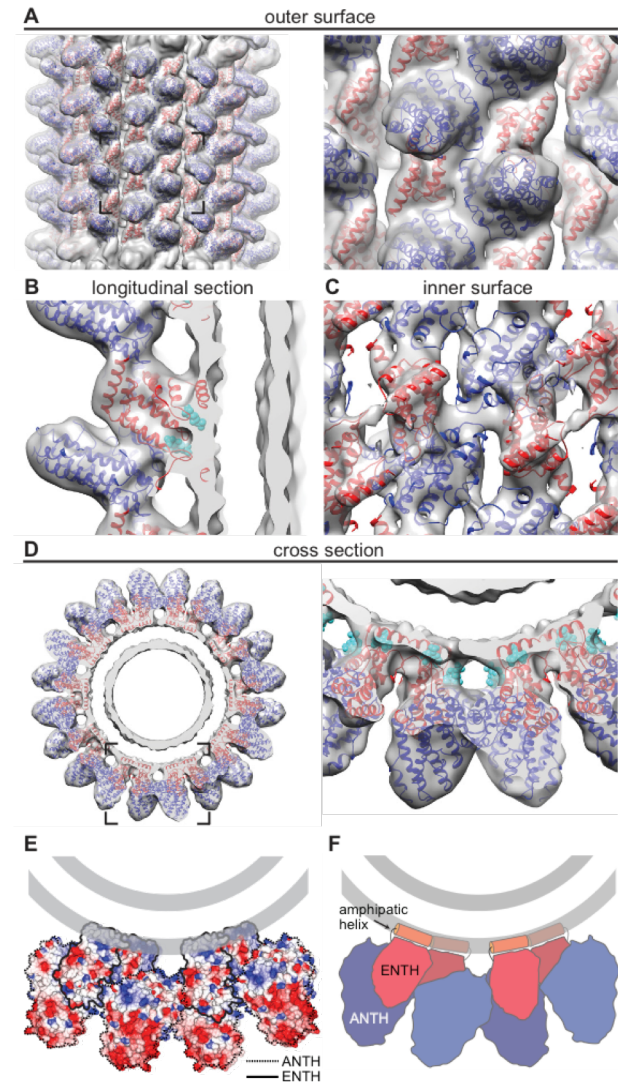
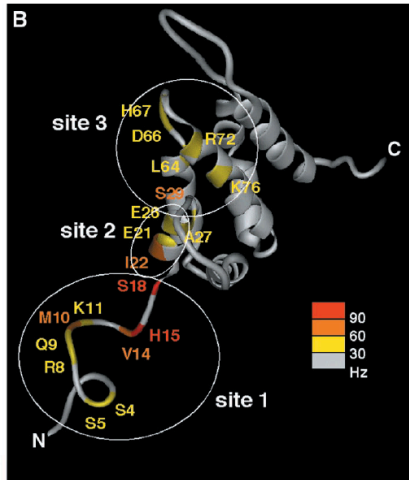
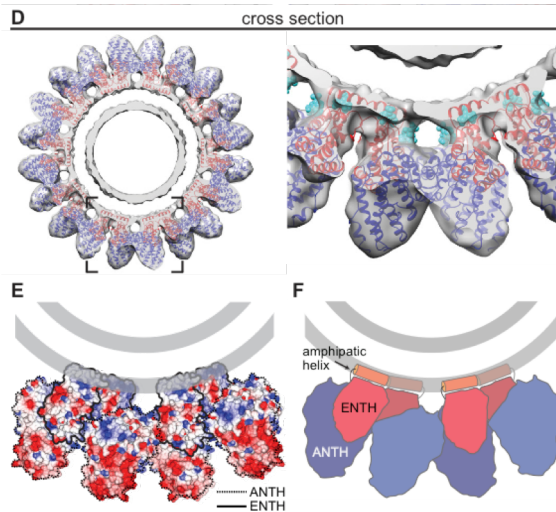
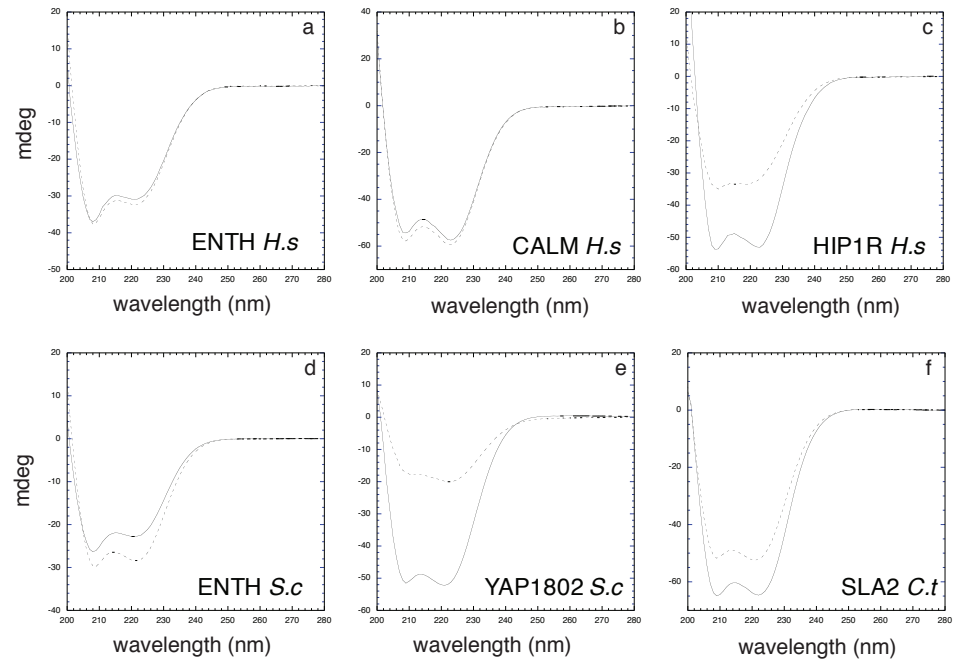


Figure 4

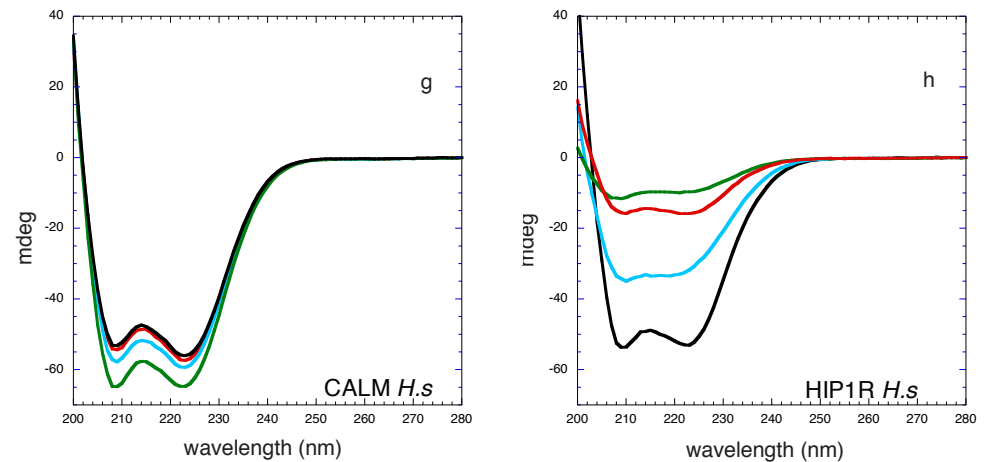
# Far-UV CD spectra of ANTH and ENTH domains



Itoh *et al.*, Science, 2001 vol 291 pp1047

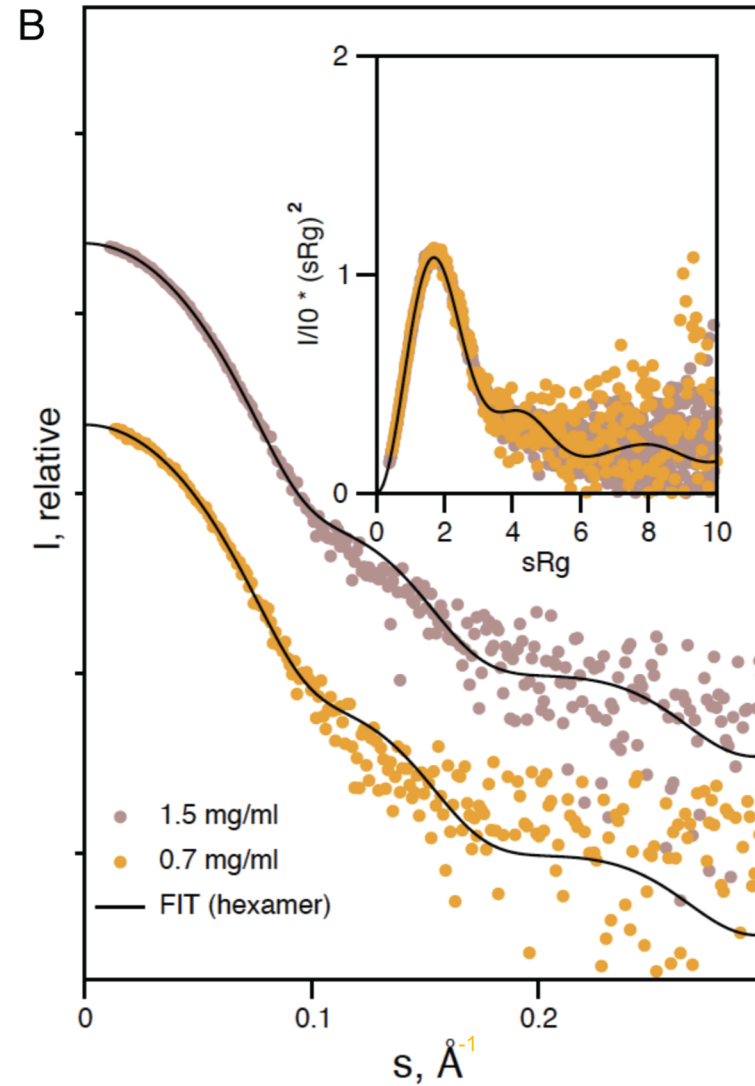
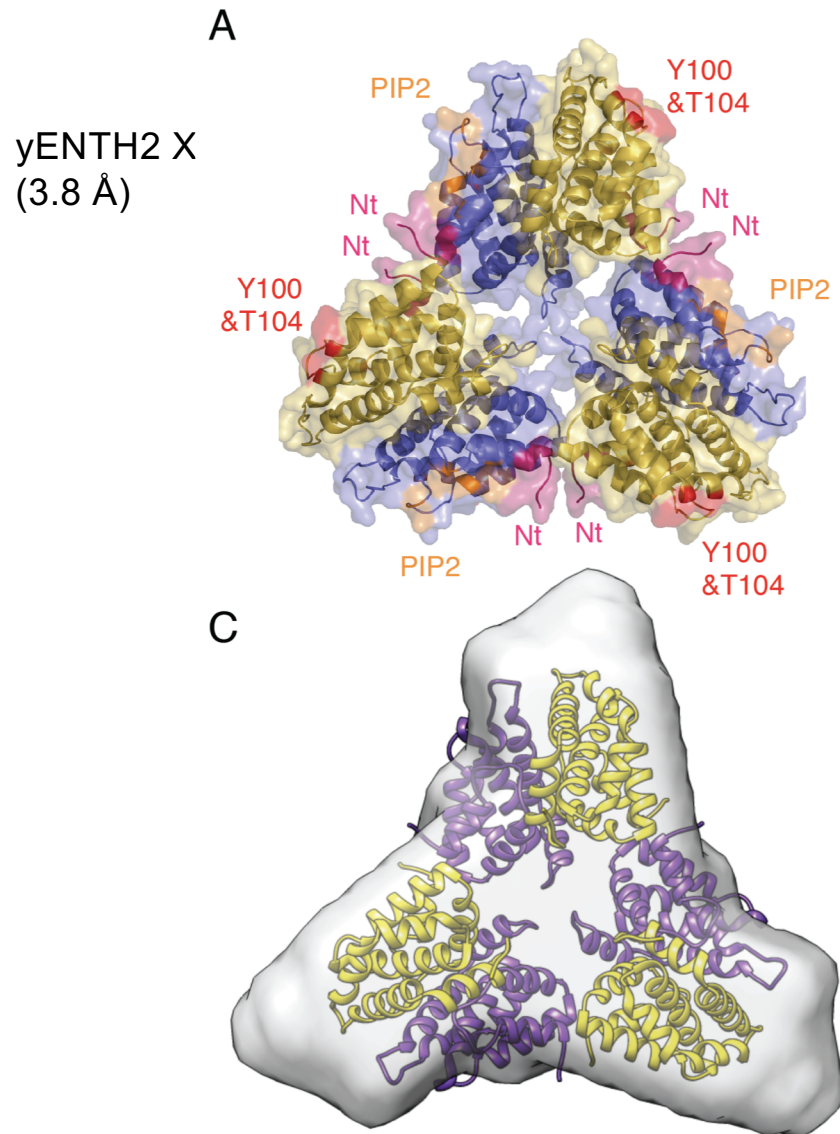


Skruzny *et al.*, Developmental Cell, 2015



Garcia-Alai *et al.*, Nature Commun, 2018 vol (1) pp. 328

# The ENTH core is conserved from yeast to humans



**SAXS**  
-The  
human  
ENTH core  
in solution

# Summary

---

- **ENTH** could adopt **different oligomeric states** when binding PIP2  
**Crystal structures & DLS**
- We showed the **structural differences between** the **CALM** and **Hip1R** subfamilies of ANTH domains **CD**
- We show the **EANTH** complex occurs in **yeast, thermophiles** and **humans ITC & NMS**

# Thank you!

## Acknowledgements:

### IMPs Project

Vadim Kotov  
Thomas C. Marlovits  
([UKE](#), [CSSB](#))  
Kim Bartels  
Christian Löw  
([EMBL](#), [CSSB](#))  
Katharina Veith  
Inokentijis Josts  
Henning Tidow  
([Uni HH](#))  
Udaya Subhramanyam  
Jörg Labahn  
([Jülich](#), [CSSB](#))  
Isabel Moraes  
([National Physical Laboratory](#), [UK](#))

## The Team



Stephan Niebling

Angelica Struve

Lucas DeFelipe

Javier Lizarrondo

Christian Günther



